Dear Dr. Ervens,

We appreciate you taking the time to consider our manuscript.

Following the suggestions of both referees, we performed several modifications in the 1D model. In the updated version, instead of prescribing the vertical velocity, it is explicitly calculated from the temperature profile, considering a positive perturbation at surface. The equation for the vertical velocity considers the buoyancy difference between the parcel and the environment, the weight of the condensate and the drag effect of the air in the neighbourhood of the ascending parcel, which includes the effect of the entrainment. The entrainment is parameterized according to the lateral inflow in a vertical jet of radius $R(t,z)$. This process modifies the temperature, humidity and aerosol content inside the parcel. Also, we introduced bins for the aerosol size distribution, and applied a documented methodology to estimate the initial bin for each droplet following activation.

In order to analyze the effect of those approaches, according to the suggestions of the referees, we repeated the simulations for different profiles and physical assumptions. To reflect the new results obtained, the structure of the manuscript was modified. We now present the results of the simulations in three different situations: including a parameterized entrainment and bin for the aerosols, excluding the parameterization of entrainment. and considering the previously employed bulk approach for the aerosols. The first situation is presented as a base case, and a detailed discussion about the corresponding results is addressed in the manuscript. Following, an additional section was introduced to compare the results from the three situation, including new figures.

We believe the manuscript has been benefited from these modifications. In addition to the sensitivity analysis, it now provides a measure of the effects of the physical assumptions considered in the model, in the context of investigating the aerosol-cloud interactions. We hope the modifications that were introduced in the manuscript contributes to provide a better insight into the cloud physics process.

On behalf of all co-authors,

Yours sincerely,

Lianet Hernández Pardo

(Comment) In the manuscript by Pardo et al., the Authors perform a series of simple model based sensitivity tests on aerosol-cloud interactions, with the intention of mapping the sensitivity of cloud properties (number of droplets, droplet size) to several parameters describing the aerosol population. The modelling work is performed with a sectional cloud microphysics scheme coupled to a 1-dimensional column model, which is driven by initial conditions representative of those in the Amazon region and an idealized vertical velocity profile.
Basically, the analysis appears sound, revealing the importance of several aerosol parameters to key cloud microphysical properties. While this is all very interesting, my primary concerns are about the representativeness of the results and the modelling methods used to produce the data for this purpose. Indeed, the Authors state that the 1-d model (the KiD kinematic driver) is designed mainly for testing microphysical schemes with a consistent kinematic framework. This is true, and in my opinion, it cannot account for important cloud dynamical responses to aerosol perturbations, which we by now know are essential to really understand the aerosol effects on clouds, particularly so in convective cumulus clouds. In particular, I find it rather surprising that the Authors do not consider e.g. how entrainment would affect their results. To back up the representativeness of the results compared to actual clouds, the importance of the dynamics should be somehow evaluated. This would most likely require at least a major review before being published in ACP. I will try to outline my concerns in more detail in the specific comments below.

(Answer) We would like to thank Anonymous Referee #1 for revising our manuscript and suggest improvements. The questions raised were very useful and helped us to consider key aspects in the methods employed and in the analysis of the results. We hope the modifications that were introduced in the manuscript, as a consequence, contributes to provide a better insight into the aerosol-cloud interactions. For practical purposes, we provided a detailed explanation of the modifications implemented in the model, in the introduction of the response to Anonymous Referee #2. In this document we provide responses to the issues raised in the review.

1. (Comment) First and foremost, how do you justify using a simple 1-d model, which obviously cannot treat e.g. effects of entrainment, to study aerosol effects on highly dynamic convective cumulus clouds? I agree that you can capture the purely microphysical response with this system (that's what it is designed to do). Even though this is interesting to an extent, I think the results from this setup describe the functionality of the microphysics scheme instead of telling us what we should expect to observe in reality (which can be very different things).

(Answer) We agree the modelling approach employed in this work is highly simplified. In real clouds, there is a much larger variety of process that could enhance or reduce the range of sensitivities that are demonstrated here. Full dynamical models, on the other hand, include many dynamics feedbacks and several subgrid processes that improve the realism of the simulations and provide a more trustable response to aerosol perturbations. However,

performing such a large set of simulations with detailed microphysics and high resolution models is computationally challenging and the interpretation of the results less straightforward. Most of the previous studies using a large subset of simulations have been performed with simple models, such as the adiabatic cloud parcel model of Feingold (2003), Reutter et al. (2009) and Ward et al. (2010).

Although the KiD was designed mainly for testing microphysical schemes with a consistent kinematic framework, without a complete representation of the physical processes other than microphysics, different idealized cases (small cumulus, stratocumulus, deep convection, etc) were elaborated to match observations of real clouds. It is common practice to use idealized cases to understand the responses of the system to different situations, ie., sensitivity tests. The KiD, in particular, was also previously used to analyse physical problems like ice nucleation (Field et al., 2012; Herbert et al., 2015) and aerosol-cloud interaction (Gettelman, 2015).

In our study, we reproduce an idealized cumulus from observed profiles of potential temperature and humidity, using in-situ aircraft observations as a reference. The results of our simulations are found to be consistent with the observations from aircraft penetrations on the top of growing convective clouds over the Amazon, performed in the same day of the sounding used to initialize our model (Cecchini et al., 2017b). Figure RR1 shows the evolution of the cloud-top DSD in the phase-space of the parameters of the gamma function for the observation and the simulation (using the original configuration of the model).

(a)   (b)
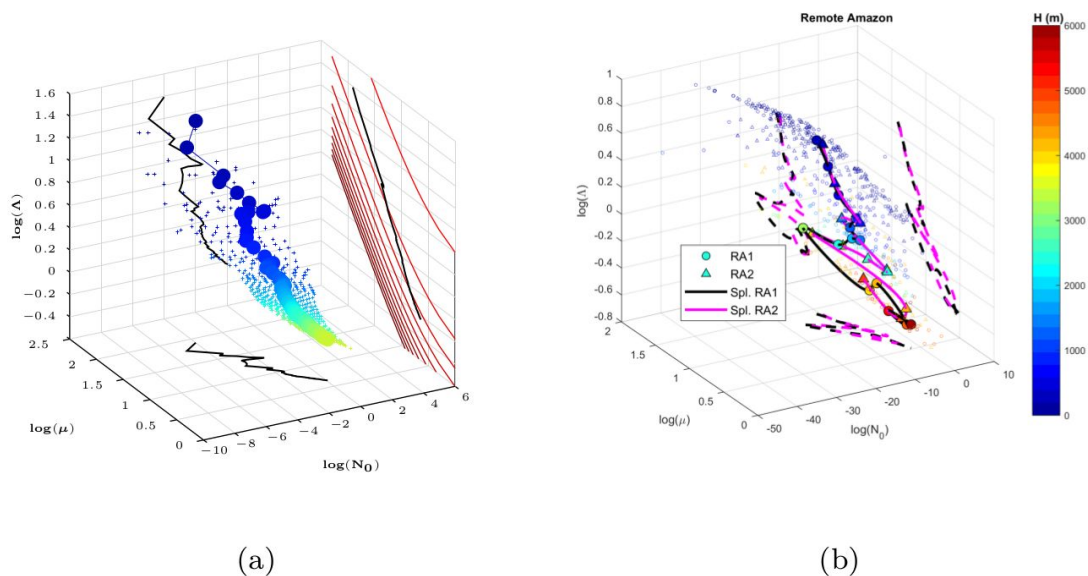
Figure RR1. Gamma phase space representation of cloud-top DSDs for different cloud widths: (a) bin microphysics simulation and (b) observation (Fig. 6 of Cecchini et al., 2017b). Small markers represent 1 Hz data, while larger ones are averages for every model level in the simulation and for 200 m vertical intervals in the observation. The color scale represents the height above the cloud base in meters. Projections on axis planes are represented by black continuous lines, in the simulation, and dashed lines, in the observation. The red lines in (a) are the projections of the surfaces with constant D_{eff}, increasing from top to bottom.

The differences in absolute values between the graphics from Fig. RR1 are determined by many factors. First, when dealing with the modeled cloud, the boundaries can be quantitatively defined; thus, there is more control over the path that follows the top of the

cloud, as well as the position of the cloud base. Consequently, the initial portion of the graphic that represents the simulation includes information about the very beginning of the cloud, when the first droplets are activated and occupy only one or two bins of the DSD (leading to larger values of μ), while in the graphic that corresponds to the observation, the first DSDs plotted (lower heights above cloud base) correspond to a more developed stage of the cloud. This is why the simulated trajectory looks like an expanded version of the warm portion of the observed one. However, the qualitative similarity between the simulated and observed trajectories is quite remarkable.

The description of the environmental conditions modulates the simulated DSD evolution and is also responsible for similarities and differences between the observed and simulated warm cloud evolution. For example, changes in the initial aerosol concentration can modify the position and shape of the simulated Gamma phase space trajectory by increasing the values of Λ and N_0 as an expression of more numerous droplets and narrower DSDs. Our sensitivity calculations agree with the calculations of Cecchini et al. (2017a), which use the measurement of the ACRIDICON-CHUVA field campaign at locations with different exposure to anthropogenic aerosol over the Amazon (this comparison is detailed in the response to Anonymous Referee #2).

In order to complement the results already shown in the manuscript, we introduced several modifications in the model, including the treatment of the dynamics and a parameterization of the effect of the entrainment and mixing (a more detailed explanation is provided in the response to Anonymous Referee #2). These new simulations provide an interesting assessment of the effect of increasing the complexity of the process represented by the model. The results obtained from different configurations are consistent, and we believe it would improve our understanding on the importance of those physical processes to evaluate the response of models to different aerosol properties.

2. (Comment) The representation of the aerosol size distribution seems very static. I get the impression that cloud activation does not affect the size distribution shape or mean size, just the number. I think this is not a very robust assumption for a study like this. Do the model simulations assume some sort of aerosol replenishment mechanism?

(Answer) Indeed, in the original version of the model, the aerosol size distribution was static, activation and aerosol regeneration did not affect the shape of the PSD, only the total number concentration. To improve the quality of our analysis, we introduced bins for the aerosol and modified the activation and regeneration processes. This had a notable impact on the simulation, mainly due to the CCN depletion. These modifications and its impact on the results are discussed in the response to Anonymous Referee #2.

3. (Comment) Is the assumed vertical velocity profile consistent with the initial temperature profile, if you think about it in terms of releasing an actual thermal? Moreover, since also the evolution of the updraft profile in time is prescribed, do the initial temperature/humidity profiles evolve consistently with the updrafts?

(Answer) The vertical velocity profile should depend on the buoyancy force caused by the different densities inside and outside the parcel. Since the vertical velocity was prescribed in

the original version of the model, there was no need for specifying these two different temperatures. The initial temperature profile was considered to be the temperature of the parcel at any time, plus the increase of temperature due to latent heat release. Meanwhile, the water vapor mixing ratio was advected and also modified by the microphysics tendencies.

To improve the consistency between those variables, in the updated version of the model, the vertical velocity is no longer prescribed, instead, it is calculated at any time and height from the instantaneous temperature difference between the parcel and the environment. The atmospheric sounding is used to define the environmental profiles, and a constant temperature perturbation is introduced at surface, in order to cause an upward displacement. The temperature and humidity fields are then advected, as well as the aerosols and the liquid water.

Minor questions:

1. (Comment) Regarding the discussion on the role of r_a on pages 8-9: the Authors appear to specify a simple unimodal aerosol size distribution for their simulations (which is fine for this study, I suppose). However, the accumulation mode can most of the time be distinguished in observations and the accumulation mode number concentration specifically is often contrasted to the number of cloud droplets. So doesn't the apparent sensitivity on r_a really fall back to separating the specific mode number concentrations?

(Answer) In a sense, yes. However, using r_a is a better approach than simply separating the modes, as it provides a gradual relation between cloud microphysical properties and aerosol size. For parameterization purposes, for instance, it is more desirable to have the r_a and not the mode dependency.

2. (Comment) The manuscript does not really say anything about precipitation. Does precipitation form in the clouds you're simulating? If so, is the aerosol population subject to wet scavenging effects?

(Answer) The precipitation is allowed to form in the model, but the amount of rain droplets is very low, specially at cloud top, we therefore neglect the effect of aerosol washout in the simulations.

References

CECCHINI, Micael A. et al. Sensitivities of Amazonian clouds to aerosols and updraft speed. Atmospheric Chemistry and Physics, v. 17, n. 16, p. 10037-10050, 2017a.

CECCHINI, Micael A. et al. Illustration of microphysical processes in Amazonian deep convective clouds in the gamma phase space: introduction and potential applications. Atmospheric Chemistry and Physics, v. 17, n. 23, p. 14727-14746, 2017b.

FEINGOLD, Graham. Modeling of the first indirect effect: Analysis of measurement requirements. Geophysical research letters, v. 30, n. 19, 2003.

FIELD, P. R. et al. Ice in clouds experiment–layer clouds. Part II: Testing characteristics of heterogeneous ice formation in lee wave clouds. Journal of the Atmospheric Sciences, v. 69, n. 3, p. 1066-1079, 2012.

GETTELMAN, A. Putting the clouds back in aerosol–cloud interactions. Atmospheric Chemistry and Physics, v. 15, n. 21, p. 12397-12411, 2015.

HERBERT, Ross J. et al. Sensitivity of liquid clouds to homogenous freezing parameterizations. Geophysical research letters, v. 42, n. 5, p. 1599-1605, 2015.

REUTTER, Philipp et al. Aerosol-and updraft-limited regimes of cloud droplet formation: influence of particle number, size and hygroscopicity on the activation of cloud condensation nuclei (CCN). Atmospheric Chemistry and Physics, v. 9, n. 18, p. 7067-7080, 2009.

WARD, D. S. et al. The role of the particle size distribution in assessing aerosol composition effects on simulated droplet activation. Atmospheric Chemistry and Physics, v. 10, n. 12, p. 5435-5447, 2010.

Response to Anonymous Referee #2

(Comment) This is a theoretical study of sensitivities of cloud droplet size distributions to initial aerosol loading. There are two unique aspects in this study: first, the authors limit their discussions on cloud top properties only; second, the sensitivity tests are thoroughly spaced over aerosol characteristics, including total number, median size, standard deviation of a log-normal distribution, and the hygroscopicity. This is a clearly structured manuscript with adequate figures and literature overview. The conclusions agree with various previous studies using different modeling tools and/or with different parameter choices. The main limitation of the current study is the use of a highly simplified kinematic model, albeit with detailed microphysical representations. I understand that there are tradeoffs to be made in order to carry out a large number of sensitivity tests. However, there should be a much more detailed discussions listing various limitations, and their associated errors, in both the kinematic framework and in handling aerosol activation processes. In addition, I think the scientific quality of the current manuscript can be improved with additional simulations and analyses. I will detail my suggestions in the follow section. There could be significant revisions if the authors decided to carry out some of the additional sensitivity studies.

(Answer) We would like to thank Anonymous Referee #2 for taking the time to analyze our work and suggest improvements. We agree that a more detailed discussion on the limitations of the modelling approach, including additional simulations to assess the influence of its shortcomings, would improve the scientific quality of the manuscript. Following the suggestions of both referees, we performed several modifications in the model. The new simulations allowed us to analyse the behavior of the sensitivities in diverse situations, providing a new perspective to the results. We are currently modifying the manuscript hoping to provide a deeper and clearer insight on the results already shown.

In this document we provide detailed responses to the issues raised in the review, as well as a description of the new capabilities of the model.

Major points:

1. (Comment) There are significant limitations in using a kinematic model. In additional, some key aerosol activations processes in the model that have been simplified. The authors skimped some of these limitations here and there in the manuscript. However, they have missed the most important aspect of the limitation discussions, that is, how these simplifications might affect their main conclusions. This is essential if the conclusions were to be useful for understanding aerosol-cloud interactions in the real world. I would suggest that the authors add a discussion section before the conclusion, to carry out some detailed, in-depth discussions. The following is the list of my suggested topics. Some of them are more obvious than others. Some of them are totally missing in the manuscript and need careful considerations.

(Answer) In order to address the impact of the limitations in the modelling approach on the results, we have modified two key aspects in in the model: the treatment of the aerosol and the computation of the vertical velocity.

I.   Aerosol:

To better account for changes in the aerosol size distribution, we introduced a set of *19* bins for dry aerosols, with radii (*r*) between *0.0076* and *7.6 µm*, according to Kogan (1991). We consider that the total number concentration of aerosols is log-normally distributed through those bins, at the beginning of the simulation, and can vary by advection, activation and regeneration after droplet evaporation. In-cloud aerosols can also vary by entrainment, which is explained later in this document.

At a given temperature and supersaturation, the critical dry size for aerosol activation is computed from the Köhler equation (Pruppacher and Klett, 1997). The initial bin for newly nucleated droplets is assigned according to its equilibrium size at *100%* relative humidity, if $r>0.09w^{-0.16}$ (Ivanova et al., 1977), where *w* represents the vertical velocity (*m/s*). According to Ivanova et al. (1977), for larger aerosols, the initial radius of the droplet will exceed *r* by a factor of $k=5.8w^{-0.12}r^{0.214}$, due to the time these particles take to reach its equilibrium size.

This method has been extensively employed (e.g., Yin et al., 2000ab, 2005; Altaratz et al., 2008; Hill et al., 2008; Mechem and Kogan, 2008) to substitute the explicit calculation of the diffusional growth of the aerosols from its dry sizes, which has a much higher computational demand. Leroy et al. (2007) analysed the influence of a similar assumption on the liquid and ice water content and the aerosol particles, drops and ice crystal spectra simulated by a 1.5D model. He found notable consistency between both approaches, even when the bin resolution was strongly decreased, as well as a reasonable sensitivity to the initial aerosol spectra.

The described approach has two major effects on the model. Previously, the activated droplets were always assigned to the smallest bin of the DSD, thus inducing a very narrow shape and spending a longer time to grow by diffusion until the collision-coalescence rate increases. In the current version, the newly activated droplets fill several bins of the DSD, which favors the development of wider DSDs and accelerates collection processes. Also, by using bins for the aerosol, we allow the PSD to evolve freely, which has a strong impact on the results. By fixing a log-normal size distribution, the previous version of the model guaranteed the continuous supply of larger aerosols for activation. Although the number concentration of aerosols decreased according to the amount of activated droplets, the assumed log-normal shape implied the presence of particles in the right tail of the PSD, which was actually removed. In the updated version, after activation, the tail of the PSD can only be filled again if new particles are advected, entrained or replenished due to droplet evaporation.

The aerosol regeneration is included here following the approach of Kogan et al. (1995) and Hill et al. (2008). It considers that large CCN particles grow to large cloud drops, which evaporates less efficiently than small droplets. Thus, small CCN will be released before large ones. As a result, the regenerated CCN are replenished to the aerosol bins starting by the smallest activated size, until the original number concentration in each bin is attained. If the number concentration of regenerated CCN is larger than the number concentration of "missing" aerosols (considering the initial PSD), which can happen by advection of droplets

to levels different than those where they were nucleated, the "excess" of CCN will be log-normally distributed according to the initially defined median radius and geometric standard deviation. A constraint is added to this scheme to conserve the domain-averaged aerosol size distribution.

This scheme provides a reasonably way to parameterize the aerosol regeneration without using a two dimensional probability density function to track the aerosols. It does not consider the processing of the aerosols inside the cloud, therefore, it could induce errors in the activation rate in situations where the collision-coalescence process is a significant sink of small aerosols and a source of larger aerosols (Lebo and Seinfeld, 2011). However, its use is justified in our case because of the occurrence of only low rates of evaporation. This evaporation takes place right above cloud-top, due to the advection of droplets to upper, unsaturated levels. Hence, even if the collision-coalescence significantly modify the size of the aerosol particles, when partial evaporation occurs, only the smallest droplets will deactivate. The collision-coalescence effect on the aerosol size distribution would have to be considered in cases with large evaporation rates, where even large droplets, containing the largest original or processed aerosols, deactivate.

II. Vertical velocity

We introduced a new method for estimating the vertical velocity in the model. It is done by solving the simplified vertical momentum equation (Pruppacher and Klett, 1997), considering the buoyancy and the weight of the liquid water, as well as the reaction force on the parcel resulting from the acceleration of the air in the neighborhood (Turner, 1963):

$$\frac{\mathrm{d}W}{\mathrm{d}t} = \frac{g}{1+\gamma}\left(\frac{T-T'}{T'} - \mathrm{w}_L\right) - \frac{\mu}{1+\gamma}W^2 \quad$$

where $\gamma \equiv m'/2m \approx 0.5$.

and μ is the entrainment rate.

For a plume of radius $R_J(z)$, the entrainment rate can be expressed as $\mu_J = C/R_J$, where $C \approx 0.2$ is the entrainment parameter. The equation for the radius of the plume is:

$$\frac{\mathrm{d}\ln R_J}{\mathrm{d}t} = \frac{1}{2}\left[\mu_J W - \frac{\mathrm{d}\ln\rho}{\mathrm{d}t} - \frac{\mathrm{d}\ln W}{\mathrm{d}t}\right]$$

For the case with no entrainment, $\mu_J = 0$ and we also neglect the acceleration of the parcel in the neighborhood, i.e., eliminate the second term and the factor $1/(1+\gamma)$ in the first term in the right side of the vertical velocity equation.

The contributions of the entrainment in the equations for the evolution of the potential temperature, the water vapor mixing ratio and the aerosols is expressed as $\mu_J(X-X')W$, where X and X' represent the in-cloud and environment values for each one of the mentioned magnitudes, respectively.

For the purpose of representing a rising plume, we introduce a constant temperature perturbation at surface. The vertical profile of potential temperature and water vapor mixing ratio are taken from the Boa Vista sounding on 11/09/2014 at 12Z, the same as in the original tests, but no smoothing procedure is applied in this case.

The results obtained with the updated model, with no entrainment, are presented below:
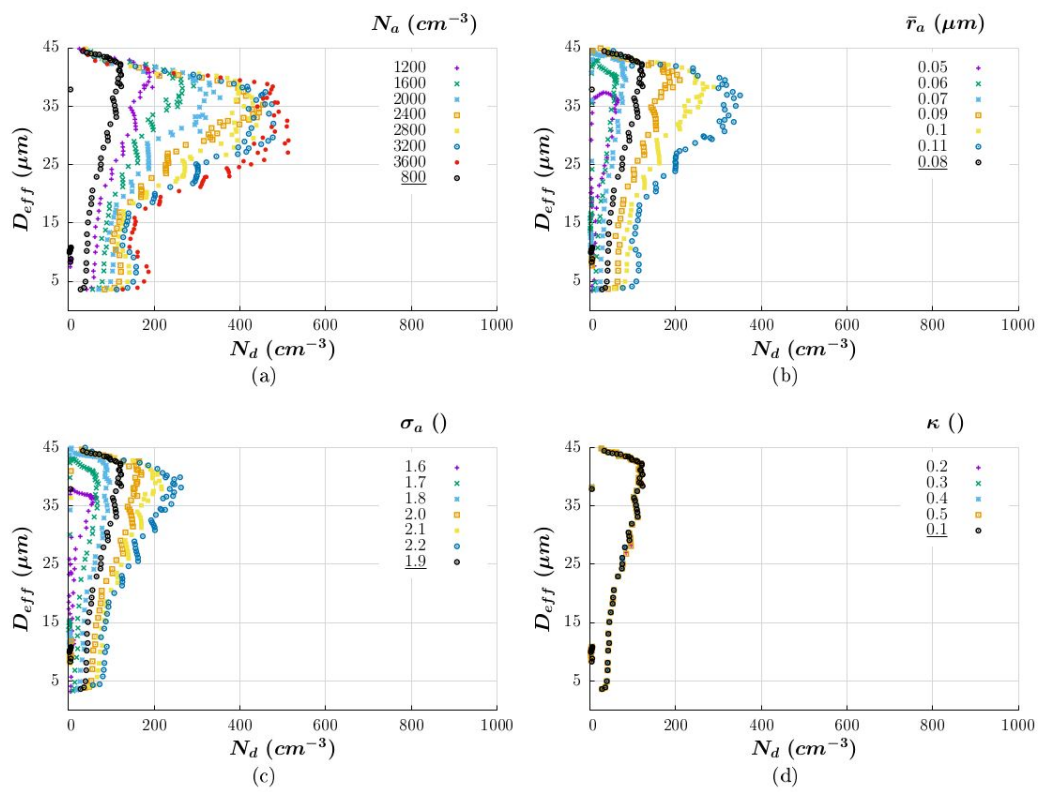
Figure R1. Illustration of the sensitivity of cloud-top bulk properties to (a) the aerosol number concentration (cm^{-3}), (b) the median radius of the aerosol size distribution (µm), (c) the geometric standard deviation of the aerosol size distribution (dimensionless), and (d) the aerosol hygroscopicity (dimensionless). The markers represent the averaged DSDs for the time steps when the cloud top remains at the same model level during its growth. The colors distinguish between simulations using different values of the parameter specified at the top of the graphs. The control simulation is represented by black markers in the figures.

Figure R1 shows a reduction of the droplet concentration (N_d) and an increase of the effective diameter (D_{eff}), compared to Fig. 3 in the original manuscript. It is a direct consequence of the modification in the treatment of the aerosol, as explained above. That is the reason why the values of the aerosol parameters are not the same than in the original tests. With the current configuration of the model, when the original values of the parameters are used, there is a very low nucleation rate and the cloud does not develop. It is reasonable, considering that once the aerosol is removed from activation, they are not spread over all sizes as in the previous version of the model, so that no more droplets are nucleated.

The trajectories in Fig. R1 keep the overall shape shown in Fig. 3 (main manuscript) until a critical point, where N_d start decreasing with height. This effect is due to the combination of two factors: the decrease of the nucleation rate and the increase of the collision-coalescence. Note that there is an inverse relation between N_d and D_{eff} at the critical

point in Fig. R1a, i.e., the smaller the aerosol number concentration, the smaller $N_{d,crit}$ and the larger $D_{eff,crit}$. It also happens in the tests with varying r_a and σ_a, but only for the values larger than the control ones. It evidences that, in the cases with smaller r_a and σ_a, the decrease of the nucleation rate due to the lack of large aerosols is the dominant factor controlling the upper part of the trajectories. The "saturation" effect that appeared in the original tests is now visible in the tests with varying aerosol number concentration, instead of the tests with the size-related parameters. It indicates the state at which all the supersaturation is consumed, and the system is therefore insensitive to the addition of more aerosols.
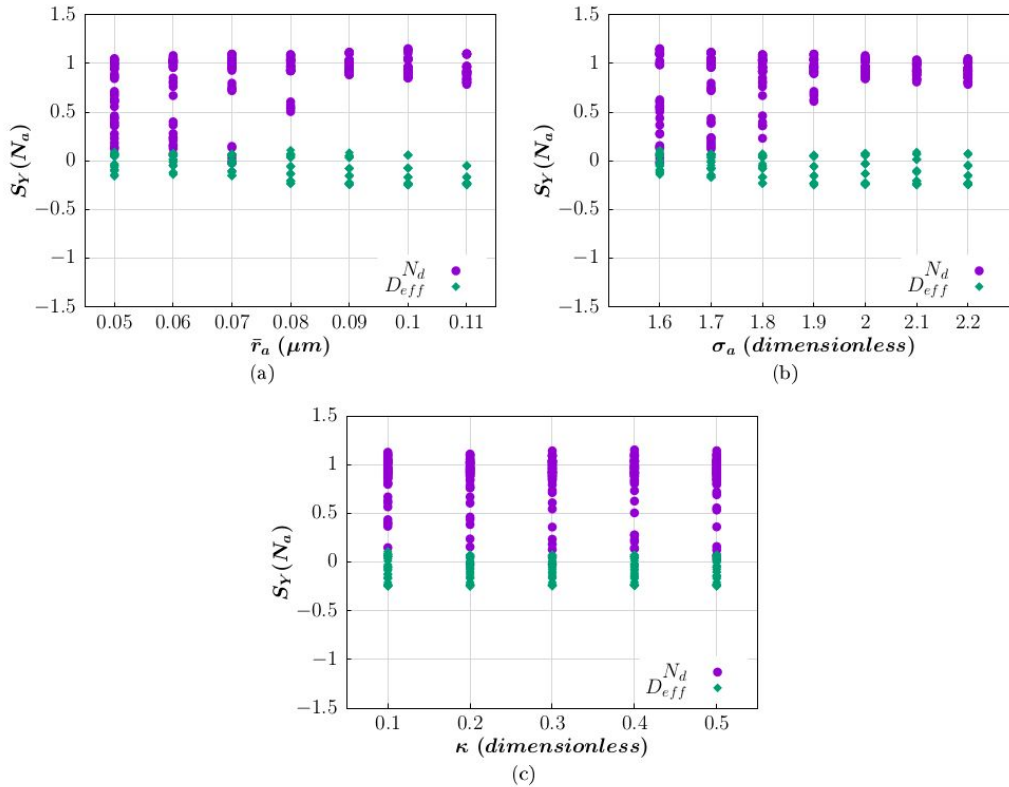
Figure R2. Sensitivities of the droplet number concentration and effective diameter to the aerosol number concentration ($S_Y(N_a)$) as a function of (a) the median radius of the aerosol size distribution (μm), (b) the geometric standard deviation of the aerosol size distribution (dimensionless) and (c) the aerosol hygroscopicity (dimensionless).

Figure R2 shows that the sensitivity of N_d to the aerosol number concentration can be almost null for small values of r_a and σ_a, while having almost no dependency on the aerosol hygroscopicity. It is consistent with the original tests, despite the difference in the values of the parameters tested. However, there is one effect that was not evident in the original tests: a secondary decrease in the sensitivity is found as the aerosol size distribution displaces toward larger aerosols and becomes wider. The latter effect is caused by the supersaturation depletion related to the enhanced activation of aerosols.

The variations in the sensitivity of the droplet effective diameter D_{eff} to the aerosol number concentration N_a are better illustrated in Fig. R3a. It can be observed that it reaches positive values for $\sigma_a = -13.3r_a + 2.7$ approximately, and decreases otherwise. These positive values

are due to absence of water vapour competition. At those points, increasing the aerosol number concentration will create more droplets (note that the sensitivity of Nd to Na is relatively high in that situation), increasing the vertical velocity by latent heat release, and therefore the supersaturation. But the increment in the number of droplets is not as intense as needed to cause a significant water vapour depletion, and since all the droplets will grow in the presence of such high supersaturations, D_{eff} is increased. On the other hand, for the smallest values of σ_a and r_a, the sensitivity is again negative. In that situation, only the largest aerosols in the right tail of the PSD are activated. Larger drops have a slower rate of growth by condensation, and the collision-coalescence rate may also be decreased due to less variety of fall speeds. Thus, even at high supersaturations, the growth of these droplets can be slower. In addition, when the total number concentration is increased and the shape of the distribution is maintained, the largest increments in the amount of aerosol occur near the center (mode values). Now, let's consider what happens in the right tail of the PSD, i.e., the aerosols that will be activated. In that situation, since the largest increments in number concentration occur toward the center of the distribution, the smaller sizes in the right tail will be favored, leading to a decrease in D_{eff} after activation. If the droplets growth rate is not as intense as to balance that trend, it will result in negative sensitivity.

Overall, Figure R3 shows that increases in both r_a and N_a have a tendency to produce lower D_{eff} (negative sensitivity). However, the effect is controlled by σ_a. For relatively narrow aerosol PSDs, increases in N_a or r_a have a lesser effect given the limited population of aerosols above the activation diameter. On the other hand, broader aerosol PSDs allow the r_a and N_a effects to go through. In the Amazon, the combination of aerosol sources (e.g. biogenic, biomass burning and urban) can lead to relatively broad aerosol PSDs, suggesting that it is more likely to find negative D_{eff} sensitivities. Cecchini et al. (2017) found an average $S_{Deff}(N_a)$ of -0.25 from aircraft measurements.
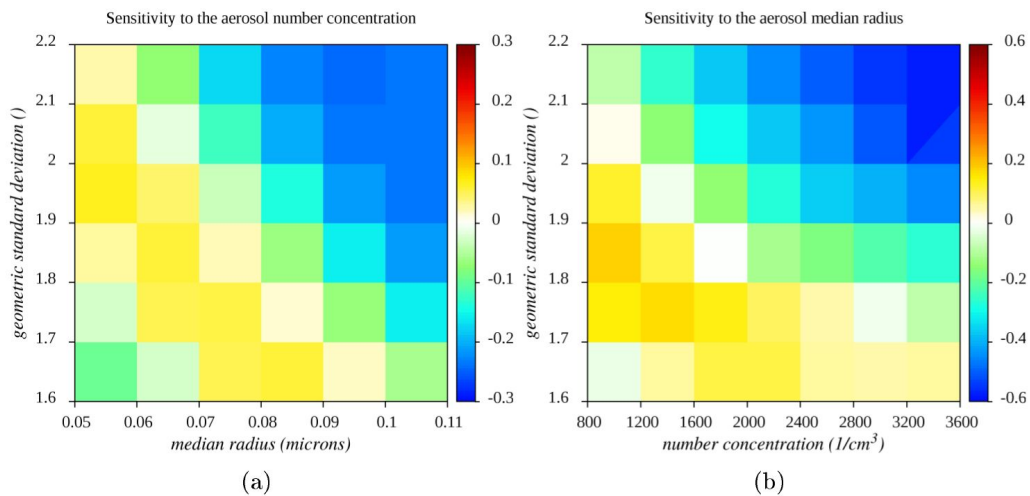
Figure R3. Sensitivity of the droplet effective diameter to (a) the aerosol number concentration ($S_{Deff}(N_a)$) and (b) the aerosol median radius ($S_{Deff}(r_a)$) as a function of other aerosol properties.

The sensitivity of N_d to the aerosol median radius (Fig. R4) increases for high values of N_a and σ_a, in agreement with our previous results, but unlike in the original test, has a very small dependency on the aerosol hygroscopicity. Also, the absolute values of $S_{Nd}(r_a)$ in this version

can be more than twice as large as in the original tests. The influence of the depletion of suitable-sized aerosols and water vapor is again visible for the smaller and larger values of σ_a, respectively, generating a maximum sensitivity at $\sigma_a \approx 1.7$. It reflects also in the behavior of $S_{Deff}(r_a)$, which response to varying Na (Fig. R3a) is similar to the response of $S_{Deff}(N_a)$ to varying r_a (Fig. R3a).

Like in the original tests, the sensitivity to the geometric standard deviation of the aerosol size distribution (Fig. R5) doubles in absolute value and shows a behavior similar to $S_\gamma(r_a)$.

The low values of the sensitivity on the aerosol hygroscopicity (Fig. R6) are consistent with its small influence on the sensitivities of the other parameters, as mentioned above. The trend of its absolute value is similar to the one in the original tests, but the sign of the sensitivities is mostly the opposite. It is reasonable, in this version of the model, because higher values of κ define smaller critical radii for activation. Although at first it would increase the droplet number concentration, it also contributes to a faster depletion of the larger aerosols, leading to a reduction in the nucleation rate afterward.
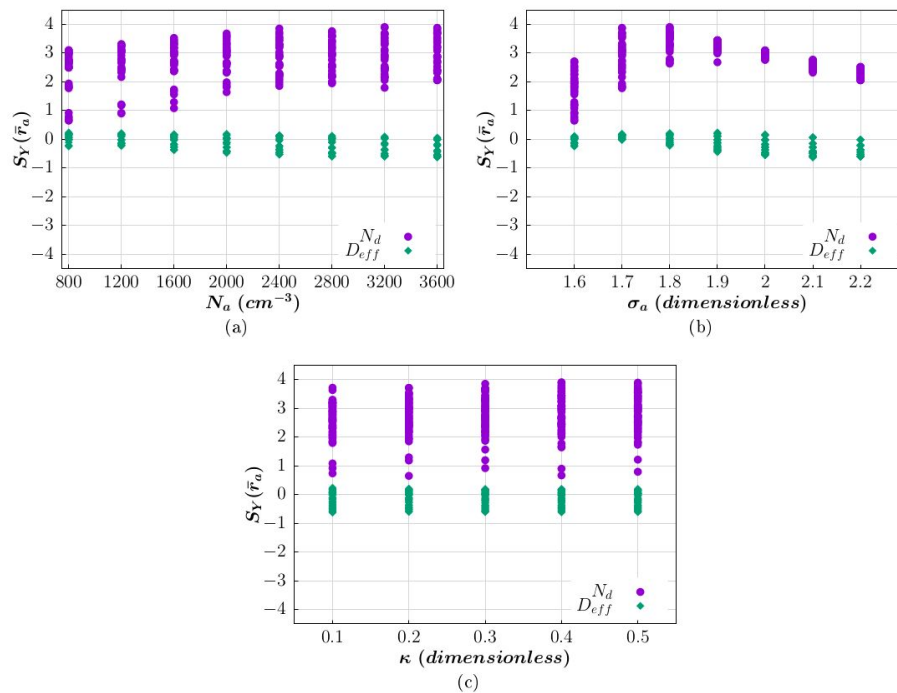
Figure R4. Sensitivities of the droplet number concentration and effective diameter to the median radius of the aerosol size distribution ($S_\gamma(\bar{r}_a)$) as a function of (a) the aerosol number concentration (cm^{-3}), (b) the geometric standard deviation of the aerosol size distribution (dimensionless) and (c) the aerosol hygroscopicity (dimensionless).
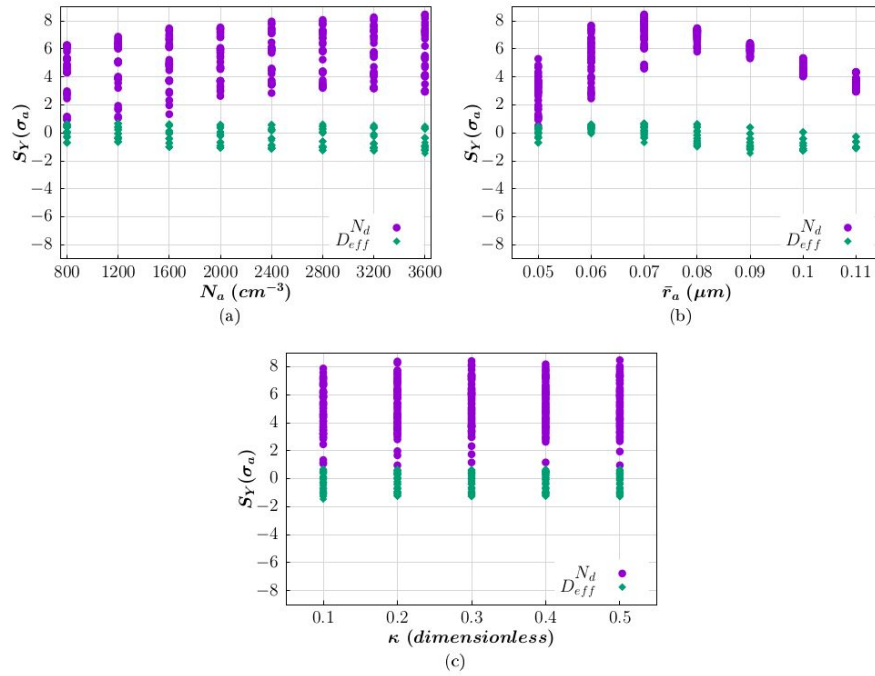
Figure R5. Sensitivities of the droplet number concentration and effective diameter to the geometric standard deviation of the aerosol size distribution ($S_Y(\sigma_a)$) as a function of (a) the aerosol number concentration (cm⁻³), (b) the median radius of the aerosol size distribution (μm) and (c) the aerosol hygroscopicity (dimensionless)
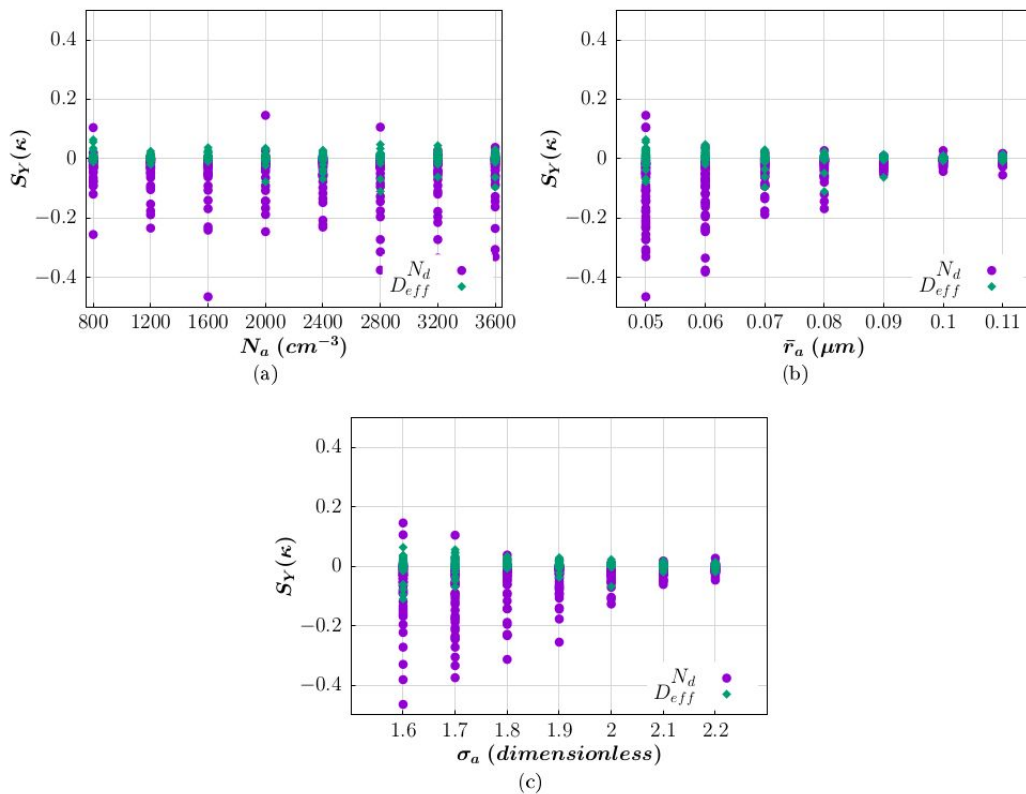
Figure R6. Sensitivities of the droplet number concentration and effective diameter to the aerosol hygroscopicity ($S_Y(\kappa)$) as a function of (a) the aerosol number concentration (cm⁻³),

(b) the median radius of the aerosol size distribution (μm) and (c) the geometric standard deviation of the aerosol size distribution (dimensionless).

Finally, aiming to complete the comparison with the original tests, we computed the variability of the cloud droplet bulk properties to emulate the information in Fig. 8 in the main manuscript. Figure R7 shows that the variability of the droplet number concentration and effective diameter (represented by the size of the bars -the standard deviation- in the figure) does not present a significant dependence on the aerosol size, in this case. Instead, the variability is a function of N_d and D_{eff} on their own. In other words, the difference between both graphics resides on the position of the points -for smaller aerosols, N_d will be lower and and D_{eff} will be larger, than for large aerosols-, and that location defines their standard deviation, i.e., points located at the left upper corner in Fig. R7a have approximately the same standard deviation than points at the same location in Fig. R7b.
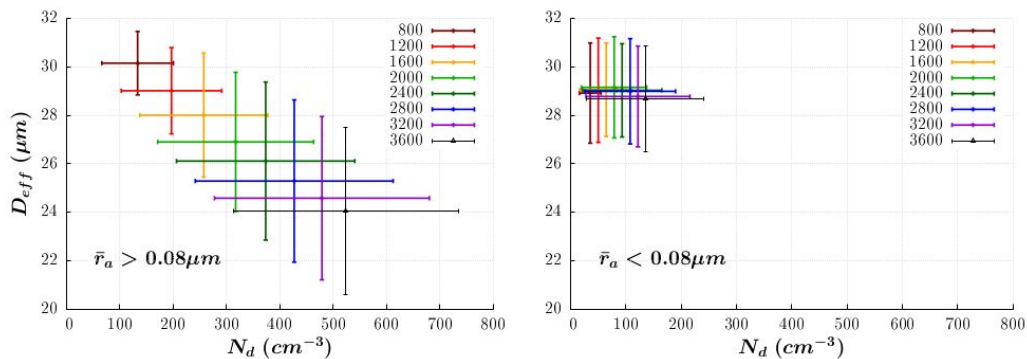
Figure R7. Mean and standard deviation of the time-averaged values of N_d and D_{eff} at the cloud top for each simulation.

a) (Comment) Will the conclusions change if a full dynamic model were used?

(Answer) The simulations performed here represent an idealized cloud resulting from observed humidity and temperature profiles and from either a prescribed or prognosed vertical velocity. The control simulation with the original version of the model was previously validated by comparing the evolution of the cloud-top against in-situ observations (see the response to Anonymous Referee #1). Also, the agreement of our results with previous studies regarding the sensitivity to aerosol properties indicates some reliability in our methodology. However, even if we assume it represent a realizable situation, corresponding to an average behavior, it does not include the variety of possibilities existing in real cases. Important processes such as turbulent entrainment and dynamic feedbacks can introduce a significant departure from the idealization we are considering, as Anonymous Referee # 2 pointed out. Full dynamical models account for dynamics feedbacks and several subgrid processes that could enhance or reduce the range of sensitivities that are demonstrated here. Nevertheless, the qualitative behavior of our main results, i.e., the dependency of the cloud sensitivity to the aerosol properties according to its position in the full parameter space, might not change. For example, Gettelman (2015) simulated

several warm rain cases with the KiD and climatological cases with a global model, using a double-moment microphysics scheme, in order to analyze the sensitivity of the aerosol-cloud interaction to cloud microphysics. They found that the test in the KiD were consistent with the global sensitivity tests. This is an aspect we intend to study in a following work, to build on the present results.

b) (Comment) If the initial sounding and/or vertical velocity profile changed, will it change the conclusions?

(Answer) In order to address this question, we performed several sets of simulations for increased/decreased values of the potential temperature, the water vapor mixing ratio and the vertical velocity using the original version of the model. The initial profiles of temperature and water vapor were modified by adding/subtracting *0.5*K and *0.5*g/kg, respectively, at all heights. The vertical velocity was modified by means of the maximum updraft speed parameter (*W* in equation 1 in the manuscript) to take values of *4*m/s and *6*m/s. For each one of this modifications, a set of simulations were performed in a way similar to the tests illustrated in Fig. 3 in the manuscript, i.e., when varying one aerosol parameter, the others were fixed at its control values. Then, we calculated the sensitivity $S_{Nd}(X_i)$ and $S_{Deff}(X_i)$ according to equation 2 in the manuscript. The results are summarized in Table 1 and Table 2 below, where the sensitivity for each condition is specified, together with the difference of the sensitivity compared to the control case ("diff" columns) and the percentage this difference represents compared to the control value ("%" columns).

Table 1. Sensitivity of the droplet number concentration to the aerosol parameters specified in the first row.

	N_a			r_a			sigma_a			kappa		
	S_Nd	diff	%	S_Nd	diff	%	S_Nd	diff	%	S_Nd	diff	%
control	1,0026			0,5464			0,3551			0,0313		
q_v-0.5 g/kg	1,0017	-0,0009	0,09	0,5048	-0,0416	7,61	0,2600	-0,0951	26,77	0,0247	-0,0066	21,05
q_v+0.5 g/kg	0,9834	-0,0192	1,91	0,6180	0,0717	13,12	0,5404	0,1853	52,18	0,0438	0,0125	39,90
Theta -0.5 K	0,9911	-0,0115	1,15	0,5926	0,0462	8,46	0,4595	0,1044	29,41	0,0395	0,0081	25,92
Theta +0.5 K	1,0004	-0,0022	0,22	0,5173	-0,0290	5,31	0,2836	-0,0715	20,15	0,0296	-0,0017	5,54
W=4	0,9867	-0,0158	1,58	0,5867	0,0403	7,38	0,5423	0,1872	52,72	0,0317	0,0003	1,01
W=6	1,0100	0,0075	0,75	0,5692	0,0229	4,18	0,3144	-0,0407	11,45	0,0314	0,0000	0,11

Table 2. Sensitivity of the droplet effective diameter to the aerosol parameters specified in the first row.

	N_a			r_a			sigma_a			kappa		
	S_Deff	diff	%	S_Deff	diff	%	S_Deff	diff	%	S_Deff	diff	%
control	-0,3522			-0,2245			-0,1433			-0,0125		
q_v-0.5 g/kg	-0,3611	0,0089	2,52	-0,2104	-0,0140	6,25	-0,0783	-0,0650	45,37	-0,0177	0,0052	41,46
q_v+0.5 g/kg	-0,3617	0,0095	2,69	-0,2518	0,0273	12,17	-0,1891	0,0458	31,97	-0,0203	0,0078	61,95
Theta -0.5 K	-0,3568	0,0045	1,29	-0,2441	0,0197	8,76	-0,1694	0,0261	18,19	-0,0151	0,0025	20,19
Theta +0.5 K	-0,3590	0,0068	1,93	-0,2136	-0,0108	4,82	-0,0930	-0,0503	35,08	-0,0137	0,0012	9,51
W=4	-0,3411	-0,0112	3,17	-0,2400	0,0156	6,93	-0,2008	0,0575	40,14	-0,0157	0,0032	25,69
W=6	-0,3617	0,0095	2,70	-0,2180	-0,0065	2,89	-0,1162	-0,0271	18,89	0,0545	0,0419	334,75

In Tables 1 and 2, the red (blue) color of cells indicates increased (decreased) sensitivity relative to the control simulation, excepting the sensitivity of the droplet

effective diameter to the higroscopicity parameter (κ) at *W=6*, to which we will refer later. Yellow cells are for percentage differences higher than *5%*, for reference.

It can be observed in the tables that the sensitivity to the aerosol concentration remains almost unaltered in all cases, with percentage differences relative to the control of less than *3.17%*. The sensitivities to the aerosol median radius and geometric standard deviation result enhanced when the water vapor mixing ratio and temperature are increased (which corresponds to a decreased potential temperature, theta), and reduced otherwise. They are also increased for smaller vertical velocities. For the larger value of the vertical velocity, the sensitivity to these size-related parameters tend to be smaller, despite the fact that $S_{Nd}(r_a)$ is larger for *W=6* than for *W=5* (control value) by a 4.18%. However, its value is still smaller than for *W=4*. Whether that behavior can be related to the existence of a minimum in the sensitivity of N_d for *W=5* is something that needs a much more detailed analysis, with a larger number of simulations for variations in *W*. Nevertheless, given the relatively low value of the percentage difference in both S_{Nd} and S_{Deff}, it can also be related to other factors in the calculations, such as those arising from the definition of the cloud-top, for example, or from the error in the fit procedure to calculate *S*. On the other hand, the sensitivities to the aerosol hygroscopicity are very small due to the values of the control parameters, as already commented in the manuscript. The influence of the variations in q_v and theta on the sensitivities to κ is the same than for the size-related parameters, except that it seems to exist a minimum of S_{Deff} at the control values of the initial profiles. As mentioned before, a deeper analysis would be necessary to understand its causes. The vertical velocity has almost no influence on $S_{Nd}(\kappa)$, but a relatively huge influence on $S_{Deff}(\kappa)$. The sensitivity of the droplet effective diameter to κ is increased by a factor of three at *W=6*, compared to its value at *W=5* (control). Also, besides increasing its modulus, it changes the sign of the sensitivity parameter, meaning that increasing the aerosol hygroscopicity would increase the droplet effective diameter. That behavior is opposite to the expected response, considering that a κ is inversely proportional to the critical radius for droplet activation. However, for a given number of aerosol particles, if the updraft is strong enough, the large rate of nucleation can deplete the aerosol content causing the supersaturation to be "used" for increasing droplet sizes thereafter. In that situation, increasing κ would accelerate the aerosol depletion, favoring the increase of D_{eff} from then on.

These tests include only a subset of the entire parameter space. To a deeper understanding of the effects of the environmental conditions on the cloud sensitivity to aerosols, it would be necessary to perform a analysis similar to that we present in the manuscript, i.e., simulate all the possible combination of the parameters values over its interval of realizable values.

We are currently performing new tests including variations in the initial profiles, with the updated version of the model. Since the evolution of the variables are better coupled now, it would be interesting to know whether the above results maintain.

c) (Comment) A small cumulus with cloud top below 6km seem to be the closest real world resemblance of the kinematic model setup. A key piece that is missing is the entrainment of environment air, together with additional

aerosols, into such a small cumulus. This is not discussed at all in the manuscript. The entrainment could come from the cloud bottom, side of the cloud, and most challenging, from the cloud top. Since the focus of this study is the cloud top properties, the variations in the cloud top entrainment along might change the existing conclusions. I think that the entrainment can be added fairly easily in the kinematic framework, with pre-determined entrainment rates and vertical variations. I suggest that the authors repeat their calculations with various entrainment rates, repeat the analysis, and see if the conclusions remain the same. I am particularly interested in how the cloud top properties change if entrainment from the top is added. I believe these additional simulations will improve the scientific quality of this study significantly.

(Answer) As explained above, we introduced a parameterization for the effect of lateral entrainment in the simulations. We consider that the column in the model is located in the center of a plume with radius $R(z)$, which mixes homogeneously with the radially entrained air at each level z. The entrainment affects the vertical velocity, the temperature, the humidity and the amount of aerosols in the column. Past studies in the Amazon have assumed that the entrainment mixing in Amazonian clouds is close to the extreme inhomogeneous case, given that the droplet effective radius remain relatively constant horizontally (e.g. Freud et al., 2011). However, the recent studies of Pinsky et al. (2016) and Pinsky and Khain (2018) indicate that homogeneous and inhomogeneous mixing can be indistinguishable for polydisperse DSDs, especially for wide distributions. Additionally, those studies show the inadequacy of previous in-situ techniques to identify mixing type. Based on this finding, we will stick to the homogeneous case in the present study as a first approximation. Further studies would be needed to assess the effects of inhomogeneous mixing and this comparison is beyond the scope of this manuscript.

Some cloud-top mixing is resolved in the model grid. However, it can be affected by the numerical diffusion and dispersion introduced by the scheme that solves the advective terms. In the updated version of the model, we use the Lax-Friedrichs first order, conservative scheme to compute the advection of temperature, water vapor and aerosol, and the ULTIMATE scheme to solve the advection of hydrometeors. A first order upwind scheme is used for solving the vertical velocity equation. The choice of the schemes was done by trial and error, in an attempt to minimize the cloud-top dispersion. However, the representativeness of the mixing induced by such an advection at cloud top must be analyzed carefully, and is out of the scope of this paper. For now, we limit our analysis to the results with and without lateral entrainment, as a proxy for the effect of the dilution caused by mixing with the air in the neighbourhood of the clouds.

Since the entrainment decreases the buoyancy of the rising air, including this process significantly reduces the cloud-top height. In order to obtain a thicker cloud, we increased the temperature perturbation at surface, compared to the no entrainment simulations.
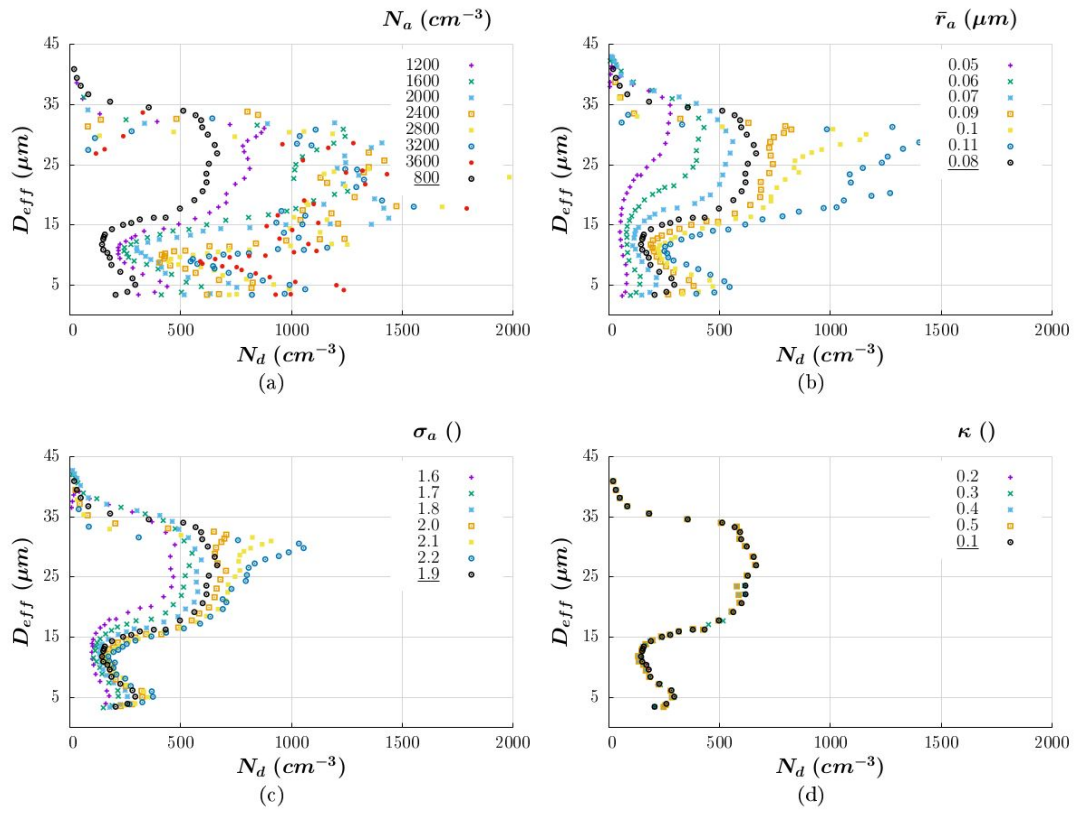
Figure R8. Similar to Fig. R1 but for the tests with entrainment.

Figure R8 shows the cloud-top trajectories for several combinations of the aerosol properties in the case including the entrainment. Compared to the no-entrainment cases (Fig. R1), there is an increase of N_d and a decrease of D_{eff}, better approaching the behavior reflected in the original tests. The inverse relation for N_d and D_{eff} at the critical point (point where there is a change in the monotonicity of N_d) holds for all the combinations of the size-related parameters, which evidences the neutralization of the aerosol depletion effect in this case.
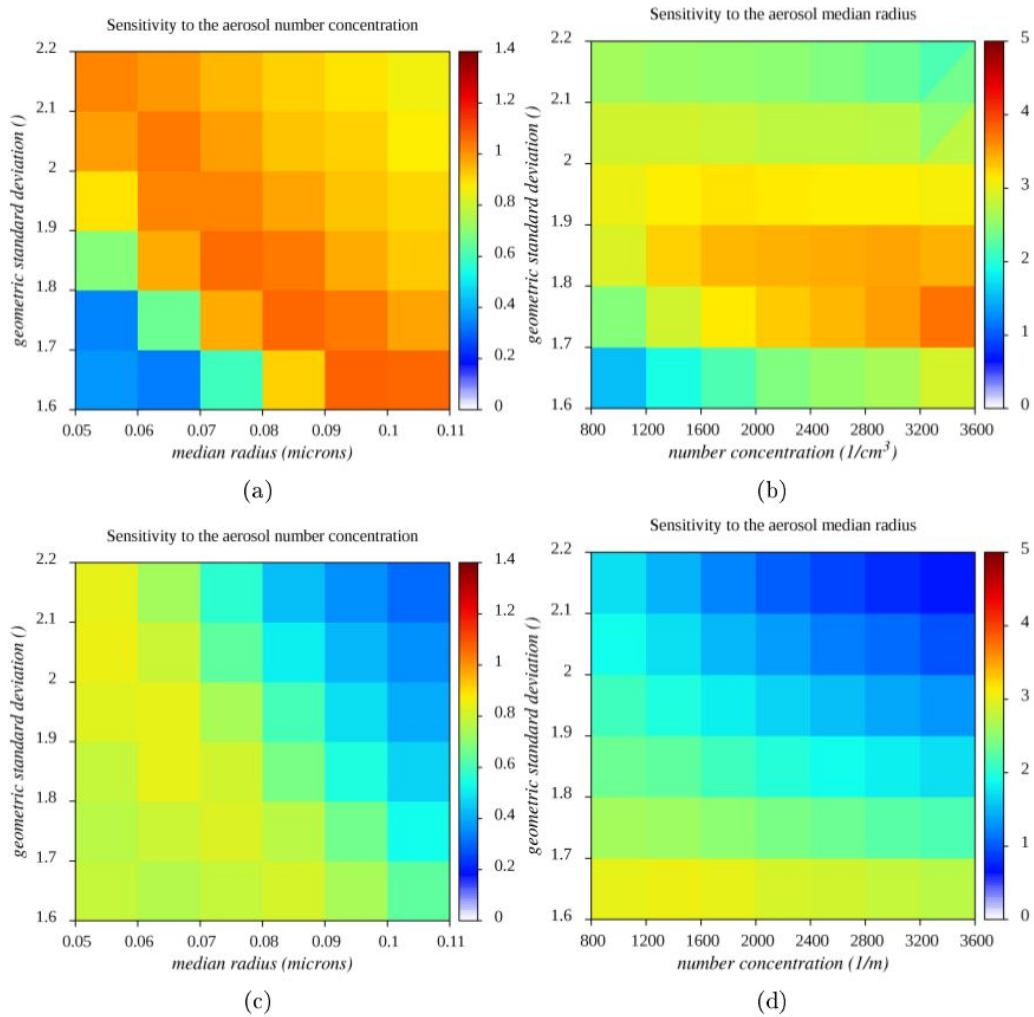
Figure R9. Sensitivity of the droplet number concentration to (a, c), the aerosol number concentration ($S_{Nd}(N_a)$) and (b, d) the aerosol median radius ($S_{Nd}(r_a)$) as a function of the other aerosol properties. (a,b) tests without entrainment, (c,d) tests with entrainment.

In Fig. R9, it can be seen that the effect of the entrainment in the sensitivity to the aerosol properties is to change the relative importance of the aerosol and water vapor depletion effects. In the no-entrainment case (Fig. R9a,b), the effect of the aerosol depletion predominates over the effect of the water vapor depletion, for smaller-sized and less numerous aerosols. On the other hand, the effect of the consumption of the supersaturation by large, numerous aerosols, is more evident in the case including entrainment (Fig. R9e,f). It is caused by both the increase of nucleation and the mixing with the entrained, drier air. In that case, even small, sparser aerosols do not cause a significant reduction of the sensitivities, because of the supply of aerosols by entrainment.
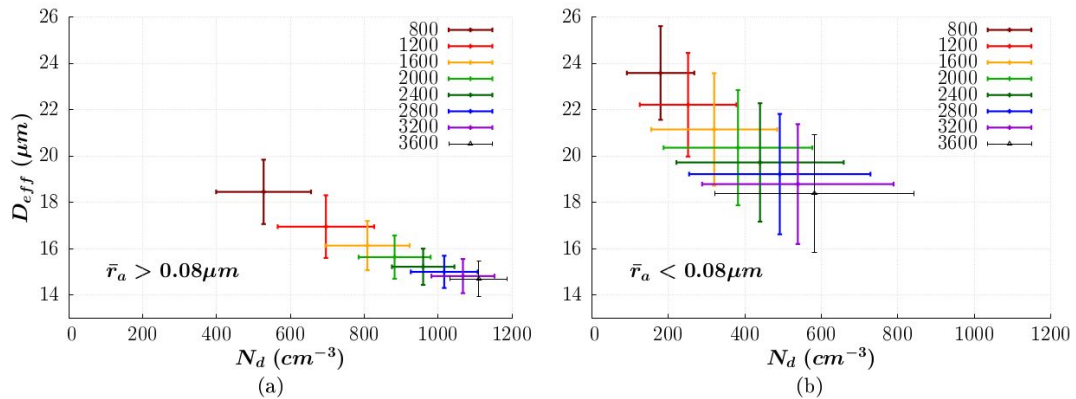
Figure R10. Similar to Fig. R7 but for the tests with entrainment.

Figure R10 illustrates the variability of the bulk properties of the droplet size distribution for the tests with entrainment. It shows that, in a better agreement with the original tests, the variability of Nd and Deff is considerably larger for the simulations with smaller aerosols.

d) (Comment) Prognostic aerosol activation is another significant limitation of the current study. On P4, L24, the authors stated that they use "a 0.25 factor that attempts to accommodate for the fact that not all CCN will grow to the size of the first droplet bin." Please discuss in details how the factor of 0.25 was chosen, how this factor could affect aerosol activation and cloud droplet spectra, and how it will affect the sensitivities.

(Answer) We agree that we were not clear about its meaning, origin and importance. We limited to just mention it, considering that it is a feature of the parameterization (Stevens et al., 1996). We also didn't express its function correctly, in order to do so, it is necessary to clarify that this artifice only applies to the mass increment in the first bin, not to its number concentration. The mass of each bin is a key feature in the TAU scheme, since it employs the method of moments for the calculations of vapor deposition and collection. However, given that the first bin contains very small droplets, the application of this factor does not significantly influence the results. In the new version of the model, the mentioned factor is not considered.

e) (Comment) Since aerosols are represented prognostically, there is no sink term for them in the microphysical calculations. In reality, aerosols are removed in clouds through both activation and wash out. Please discuss how this simplification will affect the conclusions.

(Answer) As explained earlier in this document, in the original version of the model, the total number concentration of aerosols was modified by activation, advection, and regeneration although fixing its size distribution. In the updated version, the introduction of bins for the aerosol number concentration allows to represent the evolution of the aerosol size distribution as well, and aerosols are also modified by

entrainment and mixing. Washout is not included, since the amount of precipitation produced in the simulations is negligible.

f) (Comment) Aerosol sizes also grow with increasing supersaturation, and consume certain amount of water vapor supply. This is not considered in the model. How important is this process?

(Answer) The consumption of water vapor by pre-activated aerosols is not considered in the model. The only sink of water vapor we consider is the droplet activation. We assume that aerosols smaller than the activation size don't represent a significant sink of water vapor, given the great availability of humidity over the Amazon.

2. (Comment) There are significant vertical variations in simulated cloud properties, as shown in Fig. 2. It will be beneficial to conduct the same sensitivity calculations in Fig. 3 for vertically averaged cloud properties, and compare them with the cloud top properties. The results can also be compared with Cecchini et al (2017).

(Answer) Cecchini et al. (2017) used the measurements of aircraft penetrations at the top of growing cumulus to analyse the sensitivity of the droplets population to the aerosol loading, vertical velocity and cloud-top height (taken as a proxy for cloud evolution).

In order to compare our results with Cecchini et al. (2017), we calculated the sensitivity of N_d and D_{eff} to the aerosol number concentration at intervals of 200m above cloud base (H). For consistency with their results, we consider the average and standard deviation of the sensitivity values for all the subsets (H, r_a, σ_a, κ):

$S_{Nd}(N_a)=0.82 \pm 0.55$
$S_{Deff}(N_a)=-0.19 \pm 0.08$

The mean sensitivities are very close to the values reported by Cecchini et. al. (2017), although with higher standard deviations due to the much more detailed nature of the simulations as compared to the aircraft measurements.

Minor points:

1. (Comment) P2, L23: "Must of the previous studies" should be "Most. . .";

(Answer) This error was corrected in the manuscript.

2. (Comment) P3,L28: "1 s" should be "1s", so is "1200 s";

(Answer) This error was corrected in the manuscript.

3. P8, L5: "Thus the width of the aerosol spectrum can be more important for droplet activation than. . .". I don't agree with this statement.

(Answer) The intended meaning of this statement is that, since the sensitivity is higher, a given change in the geometric standard deviation of the PSD would modify the DSD more than a proportional change in the other magnitudes. However, the effect of varying a parameter will be determined by its range of possible values. As the variations in the aerosol median radius, total number concentration and composition can be larger, its impact will be more significant.

4. (Comment) Calculations in Fig. 6 have different units. One cannot compare numbers with different units.

(Answer) By definition, the sensitivity is dimensionless. That is the reason why the graphs in Fig. 4,5,6,7 can be compared between each other.

5. (Comment) Fig. 3: What is the meaning of individual point with the same color? Are they averages over certain time period, or across certain height levels, or something else?

(Answer) Same color points in Fig. 3 apply for averages of the DSDs according to cloud-top height. The text was modified in the manuscript to clarify the meaning of this graph.

6. (Comment) It will be nice if the zero lines are labeled in Figs. 4-7, so the positives and negatives can be clearly separated.

(Answer) These figures will be modified in the corrected manuscript.

References

ALTARATZ, O. et al. Aerosols' influence on the interplay between condensation, evaporation and rain in warm cumulus cloud. Atmospheric Chemistry and Physics, v. 8, n. 1, p. 15-24, 2008.

CECCHINI, Micael A. et al. Sensitivities of Amazonian clouds to aerosols and updraft speed. Atmospheric Chemistry and Physics, v. 17, n. 16, p. 10037-10050, 2017.

FREUD, E.; ROSENFELD, D.; KULKARNI, J. R. Resolving both entrainment-mixing and number of activated CCN in deep convective clouds. Atmospheric Chemistry and Physics, v. 11, n. 24, p. 12887-12900, 2011.

GETTELMAN, A. Putting the clouds back in aerosol–cloud interactions. Atmospheric Chemistry and Physics, v. 15, n. 21, p. 12397-12411, 2015.

HILL, A. A.; DOBBIE, S.; YIN, Y. The impact of aerosols on non-precipitating marine stratocumulus. I: Model description and prediction of the indirect effect. Quarterly Journal of the Royal Meteorological Society: A journal of the atmospheric sciences, applied meteorology and physical oceanography, v. 134, n. 634, p. 1143-1154, 2008.

IVANOVA, E. T. Method of parameterizing the condensation process of droplet growth in numerical models. Izv. Akad. Sci. USSR Atmos. Ocean Phys., v. 13, p. 821-826, 1977.

KOGAN, Yefim L. The simulation of a convective cloud in a 3-D model with explicit microphysics. Part I: Model description and sensitivity experiments. Journal of the atmospheric sciences, v. 48, n. 9, p. 1160-1189, 1991.

KOGAN, Y. L. et al. Modeling of stratocumulus cloud layers in a large eddy simulation model with explicit microphysics. Journal of the atmospheric sciences, v. 52, n. 16, p. 2923-2940, 1995.

LEBO, Z. J.; SEINFELD, J. H. A continuous spectral aerosol-droplet microphysics model. Atmospheric Chemistry and Physics, v. 11, n. 23, p. 12297-12316, 2011.

LEROY, Delphine; WOBROCK, Wolfram; FLOSSMANN, Andrea I. On the influence of the treatment of aerosol particles in different bin microphysical models: a comparison between two different schemes. Atmospheric Research, v. 85, n. 3-4, p. 269-287, 2007.

MECHEM, David B.; KOGAN, Yefim L. A bulk parameterization of giant CCN. Journal of the Atmospheric Sciences, v. 65, n. 7, p. 2458-2466, 2008.

PINSKY, Mark et al. Theoretical investigation of mixing in warm clouds–Part 2: Homogeneous mixing. Atmospheric Chemistry and Physics, v. 16, n. 14, p. 9255-9272, 2016.

PINSKY, Mark; KHAIN, Alexander. Theoretical analysis of mixing in liquid clouds--Part IV: DSD evolution and mixing diagrams. Atmospheric Chemistry & Physics, v. 18, n. 5, 2018.

PRUPPACHER, Hans R.; KLETT, James D. Microphysics of Clouds and Precipitation: Reprinted 1980. Springer Science & Business Media, 2012.

STEVENS, Bjorn et al. Elements of the microphysical structure of numerically simulated nonprecipitating stratocumulus. Journal of the atmospheric sciences, v. 53, n. 7, p. 980-1006, 1996.

YIN, Yan et al. The effects of giant cloud condensation nuclei on the development of precipitation in convective clouds—A numerical study. Atmospheric research, v. 53, n. 1-3, p. 91-116, 2000a.

YIN, Yan et al. Seeding convective clouds with hygroscopic flares: Numerical simulations using a cloud model with detailed microphysics. Journal of Applied Meteorology, v. 39, n. 9, p. 1460-1472, 2000b.

YIN, Y.; CARSLAW, K. S.; FEINGOLD, G. Vertical transport and processing of aerosols in a mixed-phase convective cloud and the feedback on cloud development. Quarterly Journal of the Royal Meteorological Society: A journal of the atmospheric sciences, applied meteorology and physical oceanography, v. 131, n. 605, p. 221-245, 2005.

Quantifying the aerosol effect on droplet size distribution at cloud-top

Lianet Hernández Pardo[1], Luiz Augusto Toledo Machado[1], Micael Amore Cecchini[1,2], and Madeleine Sánchez Gácita[1]

[1]Centro de Previsão de Tempo e Estudos Climáticos, Instituto Nacional de Pesquisas Espaciais, Cachoeira Paulista, Brasil
[2]Departamento de Ciências Atmosféricas, Instituto de Astronomia, Geofísica e Ciências Atmosféricas, Universidade de São Paulo, Brasil

Correspondence to: Lianet Hernández Pardo (lianet.pardo@inpe.br)

Abstract. This work uses the number concentration-effective diameter phase-space to test cloud sensitivity to variations in the aerosol population characteristics, such as the aerosol size distribution, number concentration and hygroscopicity. It is based on the information from the top of a cloud simulated by a bin-microphysics single-column model, for initial conditions typical of the Amazon, using different assumptions regarding the entrainment and the aerosol size distribution. It is shown that the cloud-top evolution can be very sensitive to aerosol properties, but the relative importance of each parameter is variable. The sensitivity to each aerosol characteristic varies as a function of the tested parameter and is conditioned by the base values of the other parameters. The median radius of the aerosols showed, showing an specific dependence for each configuration of the model. When both the entrainment and the bin treatment of the aerosol are allowed, the largest influence on this sensitivity the DSD sensitivity was obtained for the median radius of the aerosols and not for the total number concentration of aerosols. Our results reinforce that the CCN activity can not be predicted solely on the basis of the w/N_a supersaturation-based regimes. We show that all aerosol properties can have significant impacts on cloud microphysics, especially if the median radius of the aerosol size distribution is smaller than 0.05 μ m.

1   Introduction

Because of their role as cloud condensation nuclei (CCN) and ice nucleating particles, aerosols can affect the cloud optical properties (Twomey, 1974) and determine the onset of precipitation (Albrecht, 1989; Braga et al., 2017; Rosenfeld et al., 2008; Seifert and Beheng, 2006) and ice formation (Andreae et al., 2004; Fan et al., 2007; Gonçalves et al., 2015; Khain et al., 2005; Koren et al., 2010; Lee et al., 2008; Li et al., 2011). Aerosols also play an indirect role in the thermodynamics of local cloud fields through the suppression of cold pools and enhancement of atmospheric instability (Heiblum et al., 2016). However, knowledge about the characteristics of the effects of atmospheric aerosols on clouds and precipitation is still lacking and remains an important source of uncertainty in meteorological models.

Many studies have been dedicated to quantifying the effect of aerosols on clouds through sensitivity calculations, using both modeling and observational approaches. Knowing the real values of each parameter that characterize the aerosol is difficult. Also, detailed modeling of droplet nucleation implies a high computational cost. Thus, sensitivity studies intend to determine

whether the variability of some characteristics of the aerosol population can be neglected without introducing significant errors in the description of clouds.

A major debate refers to the relative importance of aerosol composition against size distribution and total number concentration (McFiggans et al., 2006). Several studies suggest that accurate measures of aerosol size and number concentration are more important to obtain a relatively accurate description of cloud droplet populations (Feingold, 2003; Dusek et al., 2006; Ervens et al., 2007; Gunthe et al., 2009; Rose et al., 2010; Reutter et al., 2009). However, other observations/simulations show that, under certain circumstances, neglecting the variability of the aerosol composition prevent realistic estimations of the aerosol effect on clouds (Hudson, 2007; Quinn et al., 2008; Cubison et al., 2008; Roesler and Penner, 2010; Sánchez Gácita et al., 2017). This circumstantial sensitivity is commonly found in the literature and it refers not only to aerosol composition, but also to other meteorological/aerosol conditions (McFiggans et al., 2006). For instance, Feingold (2003) showed that the influence of aerosol parameters over the droplet effective radius (r_e) varies as a function of aerosol loading. Under clean condition, r_e is mostly determined by the liquid water content and the aerosol number concentration (N_a), with decreasing dependence on the aerosol size distribution (PSD), aerosol composition and vertical velocity (w). However, under polluted conditions, all of them contribute significantly to r_e. Reutter et al. (2009) obtained that the variability of the initial cloud droplet number concentration (N_d) in convective clouds is mostly dominated by the variability of w and N_a. They found that the hygroscopicity parameter (κ) appears to play important roles at very low supersaturations in the updraft-limited regime of CCN activation. Also, a significant sensitivity of N_d on the ~~aerosol size distribution~~ PSD parameters was found for ~~some situations belonging to each one of the~~ all $w - N_a$ regimes under certain conditions. Karydis et al. (2012) used a global meteorological model to obtain the sensitivity field of N_d to w, uptake coefficient, κ and N_a. They state that, overall, N_d is predicted to be less sensitive to changes in κ than in N_a, although there are regions and times where they result in comparable sensitivities.

To further evidence the importance of aerosol composition on clouds, Ward et al. (2010) consider the Reutter et al. (2009) environmental regimes but vary the log-normal median aerosol radius ($\bar{r}_a$) to examine the behavior of the sensitivity to κ. Their results compare well with the Reutter et al. (2009) regime designation when using the same value of $\bar{r}_a$. However, they show that w/N_a, or supersaturation-based regimes, cannot fully predict the compositional dependence of CCN activity, it also varies significantly as a function of $\bar{r}_a$. It is remarkable that for small aerosols ($\bar{r}_a < 0.06\mu$ m), composition affects CCN activity even in the aerosol-limited regime.

~~Most of the~~ Previous researches investigating the aerosol effect on clouds have employed adiabatic parcel models to perform multiple sensitivity calculations (Feingold, 2003; Reutter et al., 2009; Ward et al., 2010). While that approach can capture the pure response of cloud-base DSDs to aerosols through droplet nucleation and activation, it lacks the representation of the complex interactions that govern the evolution of DSDs in real clouds. Allowing to represent turbulent mixing in the models can introduce significant departure from the results obtained under an adiabatic assumption. For instance, the entrained air is expected to decrease the buoyancy of the parcel through the transfer of both sensitive and latent heat, therefore reducing the updraft velocity. The consequent reduction of the supersaturation, as well as the increased availability of unactivated aerosols can enhance the water vapor competition in the cloud. Therefore, the responses of the system to changes in the aerosol properties can suffer notable variations when turbulence and mixing is considered.

Also, most of the previous studies are based on the information from cloud-base. However, given the possibility of occurrence of cloud-top nucleation (Sun et al., 2012), it would be useful to assess the evolution of the cloud-top droplet size distribution (DSD), along with the cloud-base DSD, for exploring the aerosol first indirect effect. In a growing cumulus, the cloud-top represents the beginning of the cloud development at each level, including cloud-base ~~because~~(because, in the initial stage of the cloud life-cycle, both the base and the top coincide in space). Thus, the characteristics of the DSD at cloud-top will strongly impact the evolution of the cloud, modulating the rates of microphysical process onward and therefore determining the structure of the cloud. As Cecchini et al. (2017) pointed out, studies should take into account the altitude above cloud base. The authors showed that, on average, droplet growth with cloud evolution is comparable in absolute value and is opposite to the aerosol effect. They determined that the aerosol effect on DSD shape inverts in sign with altitude, favoring broader droplet distributions close to cloud base but narrower DSDs higher in the clouds.

Another feature that is relatively common in cloud physics modelling studies is to treat the aerosol specie as a single-moment bulk variable, i.e. considering only one bin for the aerosol number concentration, that is log-normally distributed at each grid point and time step. Thus, the growth of wet aerosols is not resolved, and aerosols with dry sizes larger than the critical size defined by the Köhler equation are immediately added to the first bin of the DSD. By fixing the shape of the PSD, those models guarantee a continuous supply of larger aerosols for activation. Although the number concentration of aerosols decreases according to the amount of activated droplets, the assumed log-normal shape implies the continuous presence of particles in the right tail of the PSD. Also, by always assigning the activated droplets to the smallest bin of the DSD, a very narrow shape is induced, spending a longer time to grow by diffusion until the collision-coalescence rate increases.

With ample water vapor supply, high temperatures and a wide spectrum of aerosol conditions, the troposphere over the Amazon constitutes an ideal scenario to study aerosol-cloud-precipitation interaction. ~~Because they belong to the "aerosol-limited regime", characterized by strong updrafts and a low aerosol background concentration (Reutter et al., 2009), Amazonian clouds~~ The Amazonian clouds that form during the wet and transition seasons are found to be very sensitive to aerosols ~~(Andreae et al., 2004; Braga et al., 2017; Cecchini et al., 2017; Fan et al., 2018; Reid et al., 1999). At the same time,~~ (Andreae et al., 2004; . Recent experimental campaigns in the Amazon have highlighted another layer of complexity in the aerosol-cloud interactions. During the wet season when the atmosphere is at the background aerosol conditions, the clouds control both the removal and production of atmospheric particles over the Amazon basin. According to Andreae et al. (2018), the production of new aerosol particles from biogenic volatile organic material, brought up by deep convection to the upper troposphere, is the dominant process supplying secondary aerosol particles in the pristine atmosphere. Then, those particles can be transported from the free troposphere into the boundary layer by strong convective downdrafts or even weaker downward motions in the trailing stratiform region of convective systems (Wang et al., 2016). During the transition or dry seasons, frequent biomass burning events change the aerosol population characteristics as a whole, not only their number concentrations. Therefore, it is important to infer the pollution effect on cloud properties and how they can interact with the natural cycle in the region.

Here we propose to explore the cloud sensitivities to several aerosol properties, by simulating some characteristics of Amazon clouds. We focus on the information from cloud-top, during the warm stages of cloud life-cycle, using a sample strategy that also includes the information from the cloud-base at the initial stage of development of the cloud. Our approach is similar

to Ward et al. (2010), but it is not limited to analyze the hygroscopicity sensitivity. Instead, we extended the discussion to the sensitivity to the aerosol median size and number concentration too, and consider their effects on both droplet size and concentration. This analysis is performed with three different model configurations that allow us to investigate the importance of representing the entrainment and mixing, as well as the evolution of the PSD, in modelling studies related to the aerosol effect.

2 Modelling approach

The ~~model employed here consists of a~~ simulations performed here employs variations of the Tel Aviv University (TAU) bin microphysics parameterization (Feingold et al., 1988; Tzivion et al., 1987, 1989) coupled to a single-column Eulerian framework~~,~~. The 1D model is based on the Kinematic Driver (KiD) (Shipway and Hill, 2012), ~~with prescribed~~ but instead of prescribing w ~~. Thus, at each time step, every grid-point parcel receives an influence from two sources: advection and microphysics processes.~~ for each time t and height z, it is calculated from the simplified vertical momentum equation, considering the buoyancy of the parcel and the weight of the liquid water, as well as the reaction force on the parcel resulting from the acceleration of the air in the neighborhood (Pruppacher and Klett, 2012):

~~The KiD prognostic variables are potential temperature () and water vapor, hydrometeor and aerosol mixing ratios (). It uses the Exner pressure as a fixed vertical coordinate and the total variance-diminishing scheme (Leonard et al., 1993) as the default advection scheme. Its prognostic variables are held on "full" model levels, while w and the density are held on both "full" and "half" levels such that the grid can be used as a Lorenz-type (Lorenz, 1960) or Charney-Phillips-type (Charney and Phillips, 1953) grid.~~

~~The KiD model was conceived as a kinematic framework to compare different microphysics parameterizations without addressing the microphysics-dynamics feedbacks. Thus, obtaining precise quantitative simulations with KiD cannot be expected; nevertheless, it can provide important insights about the responses of the simulated cloud to changes in the parameters of the microphysics scheme~~

$$\frac{dw}{dt} = \frac{g}{1+\gamma}\left(\frac{\theta - \theta'}{\theta'} - q_l\right) - \frac{\mu}{1+\gamma}w^2 \tag{1}$$

where $\gamma \equiv m'/2m \approx 0.5$, m and m' being the mass of the parcel and the mass of the air displaced by the parcel, respectively; g is the gravity acceleration; θ and θ' are the potential temperature of the ascending parcel and the environment, respectively; and q_l is the liquid water mixing ratio. The entrainment rate $\mu \equiv \frac{1}{m}\frac{dm}{dz}$ considers the lateral mass flux along the axis of a vertical plume of radius $R(t,z)$. It is assumed to follow the inverse radius dependence: $\mu = \frac{C}{R}$, where $C \approx 0.2$ is the entrainment parameter. The equation for the radius of the plume is:

$$\frac{d\ln R}{dt} = \frac{1}{2}\left(\mu w - \frac{d\ln \rho}{dt} - \frac{d\ln w}{dt}\right) \tag{2}$$

4

where ρ represents the density of the air.

In our simulations, a 1s time step was used for both dynamics and microphysics algorithms during an integration time of ~~1200~~ 1800s (~~20~~ 30min). For the vertical domain, a 120-level grid was defined with a 50-m grid spacing from 0m to 6000m of altitude.

5   As initial conditions, vertical profiles of potential temperature and water vapor mixing ratio (q_v) from an in situ atmospheric sounding [1] ~~were provided (Fig. 1a). We used the 12Z sounding,~~ corresponding to 1730Z on September 11, 2014, from ~~Boa Vista-RR, Brazil~~ Manacapuru, Brazil (Fig. 1) were provided. A constant temperature perturbation of 2.5K was introduced at surface to force the convection. ~~The sounding data were interpolated to match the model resolution and then smoothed to represent a more general situation.~~

10   ~~Here, the vertical velocity field ($w(z,t)$) was constructed based on the idea of having a layer of positive buoyancy, where a parcel updraft velocity would increase with height until reaching the negative buoyancy layer. The defined time dependence for the velocity maximum and its height roughly simulate the acceleration that the air must experience and the progressive destabilization of the air column (Fig. 1b).~~

$$w(z,t) = \begin{cases} W \sin\left(\frac{\pi}{2}\frac{t}{T}\right)e^{-\frac{1}{2}\log^2(0.004t - 0.0008z)} & (0.2z - t) < 0 \\ 0 & otherwise \end{cases}$$

15   ~~In Eq. ??, W represents the maximum updraft speed (with respect to both height and time) in and T is the length of the simulation in . The value of W was set to 5 taking into account the measurements of the ACRIDICON-CHUVA AC09 flight, where~~ The contribution of the ~~w oscillated between 0 and 8 (Cecchini et al., 2017). This flight was performed by the High Altitude and Long Range Research Aircraft (HALO) on the same date of the aforementioned sounding (Wendisch et al., 2016; Machado et al~~ ~~. It sampled the top of growing convective cumulus over remote regions of the Amazon, starting close to the local noon, in~~

20   ~~the dry-to-wet season transition~~ entrainment in the equations for the evolution of θ, q_v and N_a is expressed as $\mu(X - X')w$, where X and X' represent the in-cloud and environment values for each one of the mentioned magnitudes, respectively.

2.1   Microphysics representation

For the simulations performed in this work, we have used the TAU [1] size-bin-resolved microphysics scheme that was first developed by Tzivion et al. (1987, 1989) and Feingold et al. (1988) with later applications and development documented in

25   Stevens et al. (1996); Reisin et al. (1998); Yin et al. (2000a, b) and Rotach and Zardi (2007).

TAU differs from other bin microphysical codes because it solves for two moments of the drop size distribution in each of the bins rather than solving the equations for the explicit size distribution at each mass/size point, which allows for a more accurate transfer of mass between bins and alleviates anomalous drop growth.

In this version of the TAU microphysics[1], the cloud drop size distribution is divided into 34 mass-doubling bins with radii

30   ranging between 1.56μm and 3200μm. The method of moments (Tzivion et al., 1987) is used to compute mass and number

---

[1] http://weather.uwyo.edu/upperair/sounding.html

[1] ~~The acronym TAU refers to the Tel Aviv University, where it was primarily developed~~

[1] ~~Version available~~ Available at https://www.esrl.noaa.gov/csd/staff/graham.feingold/code/ (Accessed on: 04/11/2017)

concentrations in each size bin resulting from diffusional growth (Tzivion et al., 1989), collision-coalescence and collisional breakup (Tzivion et al., 1987; Feingold et al., 1988). Sedimentation is performed with a first-order upwind scheme. ~~Aerosols are represented by a single prognostic variable, its bulk number concentration , which is assumed to follow a log-normal size distribution. Thus, activation is calculated by applying Köhler's theory to this aerosol distribution, using a 0.25 factor that attempts to accommodate for the fact that not all CCN will grow to the size of the first bin of the droplet distribution.~~

~~One disadvantage of our approach is~~ To account for changes in the PSD, we introduced a set of 19 bins for dry aerosols, with radii (r) between 0.0076 and 7.6μ m, according to Kogan (1991). We consider that the total number concentration of aerosols is log-normally distributed through those bins, at the beginning of the simulation, and can vary by advection, entrainment, activation and regeneration after droplet evaporation.

At a given temperature and supersaturation, the critical dry size (r_c) for droplet activation is computed from the Köhler equation (Pruppacher and Klett, 2012). The initial bin for newly nucleated droplets is assigned according to its equilibrium size at 100% relative humidity, if $r < 0.09w^{-0.16}$. For larger aerosols, the initial radius of the droplet will exceed r by a factor of $k = 5.8w^{-0.12}r^{-0.214}$, due to the ~~lack of an explicit representation of the droplet activation mechanism, that would require the definition of bins to simulate the hygroscopic growth of aerosol particles. Another source of inaccuracies comes from considering only one aerosol mode with a single value of κ, ignoring quasi-internal or external mixing states (Rissman et al., 2004; McFiggans et al., 2006; Ervens et al., 2007)~~ time these particles take to reach its equilibrium size (Ivanova, 1977). The consumption of water vapor by unactivated aerosols is not considered in the model. We assume that aerosols smaller than the activation size do not represent a significant sink of water vapor, given the great availability of humidity over the Amazon.

The aerosol regeneration is included here following the approach of Kogan et al. (1995) and Hill et al. (2008). It considers that large CCN particles grow to large cloud drops, which evaporates less efficiently than small droplets. Thus, small CCN will be released before large ones. As a result, the regenerated CCN are replenished to the aerosol bins starting by the smallest activated size, until the original number concentration in each bin is attained. If the number concentration of regenerated CCN is larger than the number concentration of "missing" aerosols (considering the initial PSD), which can happen by advection of droplets to levels different than those where they were nucleated, the "excess" of CCN will be log-normally distributed according to the initially defined median radius and geometric standard deviation. A constraint is added to this scheme to conserve the domain-averaged PSD.

This scheme provides a reasonable way to parameterize the aerosol regeneration without using a two dimensional probability density function to track the aerosols. It does not consider the processing of the aerosols inside the cloud, therefore, it could induce errors in the activation rate in situations where the collision-coalescence process is a significant sink of small aerosols and a source of larger aerosols (Lebo and Seinfeld, 2011). However, ~~at first, this approach makes our results suitable to understand how changes in the aerosol properties affect the simulations of numerical models in operational or research configurations, which rarely use a detailed description of the aerosols~~ its use is justified in our case because of the occurrence of only low rates of evaporation. This evaporation takes place right above cloud-top, due to the advection of droplets to upper, unsaturated levels. Hence, even if the collision-coalescence significantly modify the size of the aerosol particles, when partial evaporation occurs, only the smallest droplets will deactivate. The collision-coalescence effect on the PSD would have to

be considered in cases with large evaporation rates, where even large droplets, containing the largest original or processed aerosols, deactivate.

3 Sensitivity analysis

We employ a phase space defined by two bulk properties of the DSD (hereinafter "bulk phase space"): N_d (~~cm^{-3}~~ cm^{-3}),

which coincides with the zeroth moment of the DSD, and D_{eff} (~~μ m~~ μ m), which is the ratio between the third and second moments.

Sensitivity tests in the bulk phase space provide a very efficient means to evaluate how a specific parameter variability can affect the evolution of cloud-top DSDs. Here, we test the sensitivity of N_d and D_{eff} at the cloud top to variations in N_a, $\bar{r}_a$, the geometric standard deviation (σ_a) of the ~~aerosol size distribution~~ PSD and κ, using ranges normally found in the Amazon

atmosphere (Gunthe et al., 2009; Martin et al., 2010; Pöhlker et al., 2016) (Table 1). There are two sets of parameters tested. The set 1 applies to the tests employing bins for the aerosol, while the set 2 is used for the simulations with a bulk treatment of the aerosol. The values of N_a, $\bar{r}_a$ and σ_a are different between both sets of parameters, because a bulk treatment of the aerosol allows the clouds to develop in the presence of smaller and less numerous aerosols, while induces unrealistic N_d values for the values in the set 1.

Table 1. Aerosol parameters used for the sensitivity tests using bin and bulk approaches for the aerosol: intervals for values and steps between them. For additional details, the reader is referred to the text.

	Set 1: bin		Set 2: bulk	
Parameter	Interval	Step	Interval	Step
N_a (~~cm^{-3}~~ cm^{-3})	$800 - 3600$	400	$200 - 900$	100
$\bar{r}_a$ (~~μ m~~ μ m)	$0.05 - 0.11$	0.01	$0.02 - 0.08$	0.01
σ_a ()	$1.6 - 2.2$	0.1	$1.1 - 1.9$	0.2
κ ()	$0.1 - 0.5$	0.1	$0.1 - 0.5$	0.1

The sensitivities were calculated as the slope of the linear fit between Y and X_i in logarithmic scale for normalization:

$$S_Y(X_i) = \frac{\partial lnY}{\partial lnX_i} \left. \frac{\partial \ln Y}{\partial \ln X_i} \right|_{X_k} \tag{3}$$

where Y represents either N_d or D_{eff}, and X_i is the aerosol property affecting Y. $S_Y(X_i)$ represents the relative change in Y for a relative change in X_i and places less reliance on the absolute measures of parameters (Feingold, 2003; Reutter et al., 2009; Ward et al., 2010). The subscript X_k indicates that when calculating the sensitivity to X_i, the other aerosol parameters are held constant. For each value at which X_k is fixed, we will obtain a new value of $S_Y(X_i)$, i.e. we can also calculate $S_Y(X_i)$ as a function of X_k ($S_Y(X_i, X_k)$).

The latter differentiates our approach from previous studies. Feingold (2003) included the variability of all $X \neq X_i$ when calculating the linear regression between ~~lnY and lnX_i~~ $\ln Y$ and $\ln X_i$, only distinguishing the results for two subsets of N_a. Similarly, Reutter et al. (2009) analyzed the sensitivities to $\bar{r}_a$, σ_a and κ for three combinations of N_a and w, but all values of Y calculated at a given value of X_i were averaged prior to fitting. This analysis was then expanded by Ward et al. (2010), who

5 calculated $S_{N_d}(\kappa)$ for different values of $\bar{r}_a$ and σ_a used to initialize the parcel model. Now, we use a more general approach that allows us to study the responses of both cloud droplet number concentration and effective diameter to changes in each aerosol characteristic, as a function of the other aerosol parameters used to initialize the model.

4 Results

The control run of the model produced a shallow cumulus that grew to 4000 m depth in about 30 minutes. Fig. 2 shows the
10 evolution of the updrafts, droplet concentration and effective diameter, characterized by the following aerosol initial parameters: N_a =800cm^{-3}, $\bar{r}_a$ =0.08μ m, σ_a =1.9, and κ =0.1.The cloud-top ~~was defined here~~ is defined as the last model level, from surface to top, where the droplet concentration was larger than ~~100~~ 1 per cm^3. ~~It is represented by black lines in Fig. 2. Figure 2 shows N_d, D_{eff} and the mixing ratio of cloud droplets (q_c), for the entire simulation. Note that the upward advection causes~~ Note that there is a maximum of N_d at cloud-top for all times. As droplets ascend and mix with new droplets, they grow by
15 diffusion of vapor and ~~, to a lesser extent, by~~ collision-coalescence. As a consequence, D_{eff} ~~and q_c are~~ is larger in upper levels~~at the last times of the simulation~~.

~~Firstly, we represented the cloud-top information in the~~ The bulk phase space view is introduced in Fig. 3 to discuss the ~~"isolated"~~ isolated effect of each parameter, when ~~fixing the values of the others. The control values of the parameters employed here are N_a =800cm^{-3}, $\bar{r}_a$ =0.05~~ keeping the other aerosol PSD properties constant. Overall, following the cloud-top in the
20 phase-space, two local maximums of N_d are found. The first one corresponds to the smallest D_{eff} (< 5 μm~~, σ_a =1.5, and κ =0.1.~~) and is related to the maximum in the nucleation rate. This represents the first steps in cloud formation, where the droplets are very small and there is no significant vertical cloud development. The second one, which is also the global maximum, is reached when the cloud is deeper, as a consequence of the accumulation of droplets advected by the updraft. Regardless of the N_d fluctuations, the cloud-top D_{eff} shows an overall monotonic increase with altitude, except in the end of
25 the simulation where the updraft decelerates.

Figure 3a shows the sensitivity of cloud-top DSDs to the initial concentration of aerosols. Note that an increase of ~~the aerosol concentration increases the number of activated drops~~ N_a increases N_d for the most part, as expected. ~~This~~ The nucleation enhancement induces a smaller ~~effective diameter~~ D_{eff} because of water vapor competition, ~~despite a slightly increased~~ for the same liquid water content (not shown). Thus, if the water vapor amount is kept constant, the diffusional growth for each
30 droplet is slowed. The latter manifests as a trend to the horizontal orientation ~~(in the direction of larger values of~~ in the lower portion of the trajectories in the bulk phase space, corresponding to the smallest sizes (< 10 μ m), where diffusion of water vapor is the predominant droplet growth mechanism. It is interesting to note that all profiles evolve towards similar values in their maximum N_d ~~) in the bulk phase space. For the most polluted situations,~~ and D_{eff}. This is related to a buffering effect of

the entrainment. Note that the entrainment term, in the temperature, water vapor and aerosol tendency equations, is proportional to the difference of the values of those variables between the cloud and the environment. Larger aerosol content will induce strongest modifications in the fields, thus increasing the contribution of the entrainment term. This feedback effect decreases the sensitivity of the maximum N_d and D_{eff} attained in the cloud to the aerosol loading. Also notable are the $N_d > N_a$ values

5   in the control run, which results from the vertical gradient of w shown in Fig. 2. Because the updrafts are stronger below cloud top, there is a tendency to ~~attain an almost constanteffective diameter is evidenced.~~ accumulate droplets in the layers analyzed here.

     Note that the fraction of activated droplets in the first level is similar between all simulations in Fig. 3a (close to one third of N_a), which is a reflect of all other aerosol PSD parameters being kept constant. In reality, increased pollution in the Amazon is

10   usually followed by changes in aerosol PSD shape given the different properties of background and biomass-burning or urban particles. Therefore, it is important to analyze the effects of every aerosol PSD parameter separately to fully understand the pollution effect in Amazonian clouds.

     Figure 3b ~~shows~~ and 3c show the sensitivity of cloud-top DSDs to ~~the median radius of the aerosol population~~$\bar{r}_a$ and σ_a while keeping the other parameters at their control standards. The effects of increasing ~~$\bar{r}_a$~~aerosol size and PSD width are similar to

15   the consequences of increasing N_a. ~~If we keep the aerosol size distribution shape constant (i.e. the same total concentration and standard deviation) and increase~~ By increasing $\bar{r}_a$ ~~, then~~ or σ_a, more droplets are activated because of the larger availability of aerosols with sizes above the activation threshold. Thus, nucleation increases, whereas diffusional growth decreases. The latter is visible during the entire trajectories in Fig. 3b and 3c.

     The tests in Fig. 3 evidence a type of ~~"saturation "~~saturation effect for the larger values of N_a, $\bar{r}_a$ and σ_a tested, i.e.

20   the sensitivity decreases as ~~this parameter increases. The combination of two factors explains this behavior : the water vapor availability and the position of the size distribution curve with respect to the critical radius for droplet activation (r_c)~~these parameters increase. This behavior is explained mainly by the supersaturation consumption. Even if continuous water vapor supply from the surface occurs, the ~~water vapor~~ supersaturation can be completely consumed~~in each time step~~, depending on the aerosol availability and the diffusional growth rate. If the number of activated aerosols is able to consume all the ~~water~~

25   ~~vapor that reaches a layer in a time step,~~ supersaturation, given certain z and t, an increase of its quantity will not introduce differences in the DSD. ~~Moreover, for certain positions of the size distribution curve with respect to r_c, an increment in $\bar{r}_a$ does not produce a significant impact on the number of activated aerosols.~~

     ~~Figure 3c shows the sensitivity to the standard deviation of the aerosol size distribution. In our tests, increasing this parameter also causes an increment of the droplet concentration through an enhancement of the nucleation rate. However, the effect of~~

30   ~~varying σ_a is more important at the earliest stages/lowest levels of the cloud (the extremity with the smallest values of N_d and effective diameter in each path). σ_a modifies the shape of the aerosol size distribution. Although an increase of~~Finally, Fig. 3d shows that the effects of varying κ are very small. Nevertheless, this is a result for one single combination of N_a, $\bar{r}_a$ ~~always enhances the number of activated droplets, the same does not apply to~~ and σ_a. ~~Instead, the effects of changing σ_a depend on the position of r_c with respect to the size distribution function. For certain values of r_c, increasing σ_a can induce a reduction in~~

35   ~~the number of droplets that become activated, whereas, for others, it can cause an increase of the number of activated droplets~~

(non-monotonic behavior). Given that r_c varies with height, it explains the differences in the effect of σ_a as the cloud height increases. These tests also illustrate that the sensitivity is larger for smaller values of σ_a, because the log-normal distribution shape is more sensitive to σ_a in the interval 1.1-1.5 than in 1.5-1.9.

Finally, Fig.3d shows the effects of varying κ in the simulation. Given the , i.e., the control values of the other parameters, the effect of changing parameters; according to Ward et al. (2010), the sensitivity to κ is relatively small. Nevertheless, we can see that increasing κ favors the nucleation through a decrease of r_c. As a consequence, N_d increases, whereas the effective diameter decreases.

The previously mentioned saturation effect can be identified for every spectrum of tests in Fig. 3. There is always an interval of values of the tested parameter in which the system becomes less sensitive. The latter has been discussed before in the literature; for example, can vary as a function of N_a and $\bar{r}_a$. Additionally, it is known that the sensitivity to κ increases substantially as κ decreases (Petters and Kreidenweis, 2007). However, that effect is more or less evident depending on the values of the other parameters. Hence, to characterize the sensitivity of DSDs to aerosol properties, we should explore the multiparameter space composed by all combinations of discrete values of the parameters from its interval of realizable values.

To illustrate that sensitivity variation, we calculated $S_{\bar{N}_d}(X_i)$ and $S_{\bar{D}_{eff}}(X_i)$, with X_i being N_a, $\bar{r}_a$, σ_a or κ. $\bar{N}_d$ and $\bar{D}_{eff}$ are the time averages of N_d and D_{eff} at cloud-top for each simulation, respectively. From Eq. 3, $S_{\bar{N}_d}(N_a)$, for example, is the slope of the linear fit between the values of $\bar{N}_d$ and N_a in logarithmic scale, for a given combination of $\bar{r}_a$, σ_a and κ. The sensitivity to one aerosol parameter can then be calculated a number of times equivalent to all possible combinations of the values of the other parameters in Table 1. From its definition, it follows that positive (negative) values of $S_Y(X_i)$ correspond to increasing (decreasing) Y as X_i increases. Also, $|S_Y(X_i)| = 1$ means that a given variation in X_i is accompanied by the same absolute variation in Y.

Figures 4, 5, 6 and 7 show $S_Y(X_i)$ as a function of all values of N_a, $\bar{r}_a$, σ_a and κ considered. Generally, $\bar{N}_d$ can be almost three times more sensitive to changes in the aerosol parameters than $\bar{D}_{eff}$, which stems from the mathematical definition of these physical magnitudes. Also, the results for $S_Y(N_a)$ agree with the theoretical limits referred in the literature and all sensitivity calculations include the ranges of previously reported values (Feingold, 2003; Reutter et al., 2009; Ward et al., 2010) . For each value in the x-axis of figures 4, 5, 6 and 7, there are several combinations of the other two parameters; as a result, there are several points for each value of the x-axis in the figures.

The impact of N_a on cloud droplets depends on the values of $\bar{r}_a$, σ_a and and σ_a, but does not vary with κ, as can be seen in Fig. 4. However, this dependency is stronger for the parameters that define the aerosol size distribution, For smaller values of $\bar{r}_a$ and σ_a, than for κ . Note that in Fig. 4c, varying κ has a small effect on the distribution of the points, compared to the effects of varying $\bar{r}_a$ and σ_a in Figs. 4a and 4b, respectively. The points are more dispersed for smaller $\bar{r}_a$ and σ_a and tend to $S_Y(N_a)$ reaches its maximum and presents a large dispersion. On the other hand, it tends to be concentrated around a maximum minimum sensitivity value as $\bar{r}_a$ increases. Generally, for smaller values of $\bar{r}_a$, σ_a and κ , $S_Y(N_a)$ can be almost null, i.e. no more or less droplets are being formed, nor its size distribution is being modified, regardless of the quantity of aerosol in the environment. In the vicinity of this state, the activation of droplets is being determined by the characteristics of the aerosol, instead of its number concentration. these parameters increase. Hence, for smaller aerosols, the relative importance

of the aerosol properties can be ~~opposite~~ very different to that at larger sizes. ~~To complement the previous analysis, Figures 6b and 7c evidence that the sensitivity to σ_a and κ, respectively, can be significantly increased for smaller values of $\bar{r}_a$.~~

Figure 5a shows that the sensitivity to the median radius of the aerosol population ~~increases~~ decreases for higher values of N_a ~~which agrees with Feingold (2003) and Rissman et al. (2004)~~ and for lower values of ~~σ_a and κ. Interestingly~~ σ_a. Similar to the behavior of $S_Y(N_a)$, the lower variability in $S_Y(\bar{r}_a)$ corresponds to the values of N_a ~~, σ_a and κ~~ and σ_a where the absolute value of the mean sensitivity is minimum~~, which is opposite to the behavior of $S_Y(N_a)$~~. Conversely, the effects of κ on the sensitivity to $\bar{r}_a$ are negligible (Fig. 5c).

The same applies to the sensitivity to ~~the geometric standard deviation of the aerosol size distribution~~ σ_a (Fig. 6), substituting σ_a by $\bar{r}_a$ as the independent variable in Fig. 6b. ~~However, it~~ It is remarkable that the absolute values of $S_Y(\sigma_a)$ are the highest between those analyzed here. ~~Thus, the width of the aerosol spectrum can be more important for droplet activation than the aerosol median radius, total concentration and composition. The reason for the small sensitivity evidenced in fig. 3c is the value of $\bar{r}_a$ taken as a reference there. Nevertheless, it is important to remember that, even~~ Nevertheless, even when $S_Y(\sigma_a)$ indicates having a high ~~potential impact (determined by the value of $S_Y(\sigma_a)$ in this case),~~ relative impact on $\bar{N}_d$ and $\bar{D}_{eff}$ for certain circumstances, we should keep in mind that the effect of varying a parameter ~~will be~~ is determined by its range of ~~possible~~ realizable values. For example, assuming that the maximum and minimum values specified in Table 1 determine the entire variation of the parameters in a given situation, it follows that ~~the modification of the DSD induced by a variation of 0.8~~ a 0.6 change in σ_a (an increase ratio of ~~1.72) would be smaller than the changes in droplet size and number concentration due to a 1.38)~~ could induce a 10.6 times increase in $\bar{N}_d$, while a variation of 0.06 ~~μm variation~~ μ m in $\bar{r}_a$ (~~an increase ratioof 4)~~a 2.2 increase ratio) can increase $\bar{N}_d$ 21.6 times, if we consider the maximum values of $S_{\bar{N}_d}(\sigma_a)$ and $S_{\bar{N}_d}(\bar{r}_a)$, respectively. In turn, a 2800cm^{-3} change in N_a (corresponding to a 4.5 increase ratio), would only increase $\bar{N}_d$ by a factor of 6.1 at most.

Note that $S_Y(\sigma_a)$ changes its sign ~~, which~~ as $\bar{r}_a$ increases (Fig. 6b). This is related to ~~the previously commented~~ variations in the effect of σ_a depending on the ~~position of r_c with respect to the size distribution function~~relation $\frac{r_c}{\bar{r}_a}$. Considering a log-normal PSD, the number of aerosols for which $r > r_c$, i.e., the number of activated droplets, is positively correlated to σ_a if $\frac{r_c}{\bar{r}_a} > 1$, and negatively correlated otherwise. If $\frac{r_c}{\bar{r}_a} = 1$, the number of activated droplets does not depend on σ_a. The positive values obtained by Feingold (2003) for the sensitivity of droplet size on σ_a, as well as the negative values reported by Reutter et al. (2009) for the sensitivity of droplet number concentration on σ_a should be due to the inclusion of larger ~~aerosol sizes, where those signs are predominant (see Fig. 6b).~~ aerosols, favoring the diminution of the r_c-to-$\bar{r}_a$ ratio.

~~The effects of~~ Finally, the sensitivity to the aerosol hygroscopicity is the lowest between those analyzed here (Fig. 7). Note that an increase ratio of 5 in the value of κ ~~on the sensitivity to size parameters is higher compared to its effect on $S_Y(N_a)$, i.e. the composition~~ modifies $\bar{N}_d$ by a factor of 1.38 at most. This is also consistent with its small influence on the sensitivities of the other parameters, as mentioned above. The symmetric distribution of the sensitivity with respect to the abscissas axis evidences a random impact of κ on the cloud-top DSDs here. This randomness is a reflect of the uncertainties involved in the determination of the cloud-top location, the calculation of $\bar{N}_d$ and $\bar{D}_{eff}$, as well as in the fitting procedure employed to obtain $S_Y(\kappa)$, that predominate in the presence of such low values of $S_Y(\kappa)$. However, it should be considered that the effects of the aerosol ~~can significantly affect the way droplets respond to changes in the aerosol size distribution (Figs. 5c and 6c).~~

composition can be significantly increased in conditions of weak updrafts (Ervens et al., 2005; Anttila and Kerminen, 2007; Reutter et al., 2...

~~Finally, the sensitivity to the aerosol hygroscopicity is the lowest between those analyzed here (Fig. 7). The absolute value of $S_Y(\kappa)$ is larger for higher N_a and smaller $\bar{r}_a$ and~~

5 Discussion

Despite the limited dynamical capabilities of our 1D framework, we adopted here a simplified approach to consider the mixing between the in-cloud and environment properties. We consider that the column in the model is located in the center of a plume with radius $R(t,z)$, which mixes homogeneously with the radially entrained air at each z. The entrainment affects the vertical velocity, the temperature, the humidity and the amount of aerosols in the column. Past studies in the Amazon have assumed that the entrainment mixing in Amazonian clouds is close to the extreme inhomogeneous case, given that the droplet effective radius remain relatively constant horizontally (Freud et al., 2011). However, the recent studies of Pinsky et al. (2016); Pinsky and Khain (2018) indicate that homogeneous and inhomogeneous mixing can be indistinguishable for polydisperse DSDs, especially for wide distributions. Additionally, those studies show the inadequacy of previous in-situ techniques to identify mixing type (the so-called mixing diagrams). Based on this finding, we will stick to the homogeneous case in the present study as a first approximation. Further studies would be needed to assess the effects of inhomogeneous mixing and this comparison is beyond the scope of this manuscript.

Some cloud-top mixing is resolved in the model grid. However, it can be affected by the numerical diffusion and dispersion introduced by the scheme that solves the advective terms. The representativeness of the mixing induced by such an advection at cloud top must be analyzed carefully, and is out of the scope of this paper. For now, we limit our analysis to the results with and without the inclusion of some lateral entrainment rates, as a proxy for the effect of the dilution caused by mixing with the air in the neighbourhood of the clouds. By using bins for the aerosol, we allow the PSD to evolve freely. This way, after activation, the tail of the PSD can only be filled again if new particles are advected, entrained or replenished due to droplet evaporation. Also, since the newly activated droplets fill several bins of the DSD, the development of wider DSDs is favored, accelerating collection processes. This method has been extensively employed (Yin et al., 2000b, a; YIN et al., 2005; Altaratz et al., 2008; Hill et al., 20... to substitute the explicit calculation of the diffusional growth of the aerosols from its dry sizes, which has a much higher computational demand. Leroy et al. (2007) analyzed the influence of a similar assumption on the liquid and ice water content and the aerosol particles, drops and ice crystal spectra simulated by a 1.5D model. He found notable consistency between both approaches, even when the bin resolution was strongly decreased, as well as a reasonable sensitivity to the initial aerosol spectra. We use this approach here to test the importance of including a more detailed treatment of the PSD in the model, when investigating the aerosol effect on cloud-top DSDs.

Figure 8 and 9 illustrate the behavior of the sensitivity to each aerosol parameter in three different hypothetical situations. The first column shows the results from the simulations described in the previous section, the results without entrainment are shown in the second column, and the simulations using a bulk approach for the aerosol (with entrainment) are represented in

the third column. For the plots shown in the first three lines in Figs. 8 and 9, the value of κ is fixed to 0.1. The response of the sensitivities to changes in κ are not shown because of its smaller influence compared to the other parameters. The graphs in the last line in Figs. 8 and 9 show $S_Y(\kappa)$ at $\sigma_a = 1.9$ and $\sigma_a = 1.5$, for the cases with a bin and bulk treatment of the aerosol, respectively. The variations of $S_Y(\kappa)$ due to changes in σ_a , and has a small dependency on N_a , for most of the values

5 considered here. Note that are similar to the variations due to $\bar{r}_a$, which is represented in the y-axis of the figures.

The values of the aerosol parameters in the tests without bins for the aerosols (third column in Figs. 8 and 9) are usually lower than in the previously discussed tests. The reason is that, with this configuration, when the original values of the parameters are used, there is a very high nucleation rate that leads to unrealistic values of N_d and ends up by destabilizing the model. It is reasonable, considering that once the aerosol is removed from activation, the remaining unactivated aerosols are spread over all

10 sizes, perpetuating the conditions for droplet formation. At the same time, this permits clouds to develop in conditions where there would be a negligible nucleation rate if a bin treatment of the aerosol were employed.

Figure 8b,e,h,k show that, without entrainment, $S_{\bar{N}_d}(X_i)$ is lower for low values of N_a , for the intervals of $\bar{r}_a$ and σ_a , due to a faster depletion of the aerosols of suitable sizes for activation. A secondary decrease in the sensitivity is found at more polluted situations, with larger aerosols and wider sizes distributions. The latter effect is caused by the supersaturation depletion related

15 to an increase in the amount of activating aerosols. That behavior contrasts with the responses in the entrainment case, where the lower supersaturations and the supply of additional aerosols from the environment enhance the water vapour depletion and inhibits the aerosol depletion effects.

When the entrainment is not considered, $S_{\bar{D}_{eff}}(N_a)$ reaches very low absolute values or even positive values for an intermediate interval of the independent variables, and increases its absolute value otherwise (Fig. 9b). The same behavior is shown for

20 $S_{\bar{D}_{eff}}(\bar{r}_a)$ and $S_{\bar{D}_{eff}}(\sigma_a)$ (Figs. 9e and 9h). The positive sensitivity evidences a less intense water vapour competition. At those points, increasing the N_a, $\bar{r}_a$ and/or σ_a where the absolute value of $S_Y(\kappa)$ is maximum, it is still smaller than the sensitivity to those parameters in the same interval. However, its influence can be more than 50% of the sensitivity to will create more droplets, given the positive values of $S_{\bar{N}_d}(N_a)$, $S_{\bar{N}_d}(\bar{r}_a)$ and $S_{\bar{N}_d}(\sigma_a)$ discussed above, increasing the vertical velocity by latent heat release, and therefore the supersaturation. Thus, if the increment in the number of droplets is not as intense as

25 needed to cause a significant water vapour depletion, all the droplets will grow in the presence of such high supersaturations, therefore increasing D_{eff}. Conversely, for the smallest values of N_a, which confirms that neglecting the effects of the aerosol composition is non trivial. Moreover, the effects of the aerosol composition can be significantly increased in conditions of weak updrafts (Ervens et al., 2005; Anttila and Kerminen, 2007; Reutter et al., 2009). That, in combination with the values of N_a , $\bar{r}_a$ and σ_a can determine an even more important role for κ. As Ward et al. (2010) concluded, the sensitivity decreases

30 its absolute value again or even becomes negative. In that situation, only the largest aerosols in the right tail of the PSD are activated. Larger drops have a slower rate of growth by condensation, and the collision-coalescence rate may also be decreased due to less variety of fall speeds. Thus, even at high supersaturations, the growth of these droplets can be slower. In addition, when the total number concentration is increased and the shape of the distribution is maintained, the largest increments in the amount of aerosol occur near the center of the size distribution (mode values). Now, let's consider what happens in the

35 influence of right tail of the PSD, i.e., the aerosols that will be activated. In that situation, since the largest increments in

number concentration occur toward the center of the distribution, the smaller sizes in the right tail will be favored, leading to a decrease in D_{eff} after activation. If the droplets growth rate is not as intense as to balance that trend, it will result in negative sensitivity.

In Figs. 8c and 9c it can be seen that, when a bulk approach is used for aerosols, the absolute value of $S_Y(N_a)$ increases monotonically as $\bar{r}_a$ and σ_a increase and it is not affected by the supersaturation depletion, because independently of r_c, there will always be a certain amount of aerosols such that $r > r_c$.

Also, the absolute value of $S_Y(\bar{r}_a)$ increases for higher values of N_a, which coincides with the results of Feingold (2003) and Rissman et al. (2004), and for lower values of σ_a (Figs. 8f and 9f). The same applies to $S_Y(\sigma_a)$ (Figs. 8i and 9i), substituting σ_a by $\bar{r}_a$ as the independent variable. However, the maximum value of the sensitivity to the size-related parameters is significantly decreased compared to the simulations with a bin treatment of the aerosol. $S_{\bar{N}_d}(\sigma_a)$ even reaches slightly negatives values for the larger $\bar{r}_a$ in these tests, which is related to the previously commented variations in the ~~shape parameter on $S_Y(\kappa)$ are more important for small $\bar{r}_a$. This is evidenced by the dispersion of~~ effect of σ_a depending on the position of r_c with respect to the size distribution function.

Finally, it can be observed in Fig. 8l and 9l that, when the model uses a bulk approach for the aerosol specie, $S_Y(\kappa)$ is larger for higher N_a and smaller $\bar{r}_a$, in agreement with the results of Ward et al. (2010). The figures evidence that $\bar{N}_d$ and $\bar{D}_{eff}$ are much more sensitive to κ when considering a bulk approach for the aerosols than when its size distribution is explicitly represented in the model. Note that, in the former case, $S_Y(\kappa)$ can be about 50% of $S_Y(N_a)$, which is a significant influence. However, perhaps the most relevant difference between these simulations and the ones using bins for the aerosol is the change in the sign of $S_Y(\kappa)$. Although, at first, higher values of κ would determine a smaller r_c, it also contributes to a faster depletion of the larger aerosols, leading to a reduction in the nucleation rate afterward. That is the cause for the negative (positive) values of $S_{\bar{N}_d}(\kappa)$ ($S_{\bar{D}_{eff}}(\kappa)$) obtained in the tests using bins for the aerosol (Fig. 8k and 9k). On the other hand, the ~~points for $\bar{r}_a < 0.05\mu m$ in Fig. 7b. Of course, that dispersion includes the responses to changes~~ latter has not effect on the results when the PSD is fixed, therefore positive (negative) values of $S_{\bar{N}_d}(\kappa)$ ($S_{\bar{D}_{eff}}(\kappa)$) are obtained.

Overall, our analysis shows that increases in N_a ~~too, it is not entirely caused by the~~, $\bar{r}_a$ and σ_a ~~variability. The information contained in Fig. 7b agrees with the sensitivity of droplets~~ produce higher $\bar{N}_d$ (positive sensitivity) and smaller $\bar{D}_{eff}$ (negative sensitivity) when both entrainment and aerosol bins are included in the simulations. This coincides with the results of Cecchini et al. (2017), who found cloud-top averages of $S_{\bar{N}_d}(N_a)$ and $S_{\bar{D}_{eff}}(N_a)$ of 0.84 and -0.25, respectively, from aircraft measurements over the Amazon forest.

The values of sensitivities reported by Feingold (2003); Reutter et al. (2009); Ward et al. (2010) are included in the range of sensitivities obtained here; plus the variability added by the diverse universe of situations found over the aerosol parameter space. However, comparisons between our results and previous research are not straigforward, considering the influence of the cloud evolution here. How fast is the aerosol and water vapor depletion, for example, will determine how much nucleation will occur above cloud-base. A large supersaturation can cause a fast activation rate initially, but will decrease the intensity of that process afterwards. The response to changes in ~~κ, computed by Ward et al. (2010) for the aerosol-limited regime, as a function of $\bar{r}_a$.~~ the aerosol properties in this case might be different from that with a moderate and more spatially distributed

activation rate. In the simulations with a bulk treatment of the aerosol, the aerosol depletion is slower. Thus, for a certain time interval, each cloud-top level behaves like an independent cloud base regarding the intensity of the nucleation. That explains the similarities between the sensitivities obtained from the simulations using a bulk approach for the aerosols and previous research.

From our analysis, it turns out that $\bar{r}_a$ is the most ~~important parameter , from those analyzed, that influences~~ influential parameter that determines the sensitivity to aerosols ~~. This is particularly interesting because of~~ at cloud-top, in contrast with the importance that has been conventionally attributed to the aerosol number concentration. ~~Considering this sensitivity limitation, for certain conditions, other variables, such as the aerosol median size and size distribution shape, can be more influential in determining the evolution of an air parcel.~~

~~We calculated the time-averaged values of N_d and D_{eff} for the cloud-top DSDs at each simulation. Figure ??~~ To further illustrate this, Figure 10 shows the mean and standard deviation of ~~these averages~~ $\bar{N}_d$ and $\bar{D}_{eff}$ for each value of N_a tested, at each of the above referenced situations: with entrainment and bin for aerosols (a-b), without entrainment (c-d), and without bins for aerosols (e-f). The length of the standard deviation bars ~~is determined by the ranges of~~ reflects the changes in $\bar{r}_a$, σ_a and κ. ~~Figure ??a represents the generally accepted knowledge: given a certain temperature and water vapor availability, the bulk properties of a cloud are mostly~~

For the first (and most complete) situation considered, it can be seen that the state of the system is not sufficiently determined by N_a. ~~However, this behavior seems to be valid only for the largest values of $\bar{r}_a$. If the aerosol size distribution~~, specially if the PSD is displaced to ~~a~~ smaller radius ~~(Figure ??b), then more aerosol characteristics must be specified.~~

~~Our~~ Fig. 10b). For instance, increasing N_a by a factor of 3 in Fig. 10b, from 800 cm^{-3} to 2400 cm^{-3}, there is still some overlapping between the corresponding standard deviation bars in the phase-space. However, the bars are significantly smaller if larger aerosols are considered (Fig. 10a), indicating a tendency to approach the generally accepted knowledge, i.e., increasing the importance of N_a in determining the characteristics of the DSDs. These results show that the study of the aerosol-cloud interaction must include the parameters describing aerosol properties, such as the size ~~and hygroscopicity~~ distribution, at least for ~~$\bar{r}_a \lesssim 0.05\,\mu m$~~ $\bar{r}_a \lesssim 0.08\,\mu$ m. These parameters can produce changes in the DSD as large as those caused by changes in the aerosol ~~concentration. The error associated with its misrepresentation increases with aerosol loading and can be as large as 23% in N_d and 15% in D_{eff} for $N_a = 800$ cm^{-3}, which is larger than~~ number concentration. These findings are also relevant given the current discussion about the importance of ultrafine aerosol particles in the development of deep convective clouds over the Amazon (Wang et al., 2016; Fan et al., 2018).

In turn, Fig. 10c-d show that, when the entrainment is not considered in the model, the variability of $\bar{N}_d$ and $\bar{D}_{eff}$ does not present a significant dependence on the aerosol size; it is a function of $\bar{N}_d$ and $\bar{D}_{eff}$ on their own. In other words, the location of the points in the ~~error introduced by a 25% variation in N_a, according to Fig. ??b. Note that aerosol loads larger than 800 cm^{-3} are common in~~ phase-space determines their standard deviation. Points located at the left upper corner in Fig. 10c, for instance, have approximately the same standard deviation than points at the same location in Fig. 10d. The difference between both graphics resides on the position of the points: for smaller aerosols (Fig. 10d), $\bar{N}_d$ will be lower and $\bar{D}_{eff}$ will be larger, than for large aerosols (Fig. 10c). On the other hand, the results indicate that the importance of N_a may be overestimated

if a bulk treatment of the aerosol is employed (Fig. 10e-f). It can be seen that, in this case, there is a reduction of the overlapping between the standard deviation bars, specially for larger and sparser aerosols.

The simulations performed here represent an idealized cloud resulting from observed humidity and temperature profiles. However, even if we assume it represent a realizable situation, corresponding to an average behavior, it does not include the variety of possibilities existing in real cases. Important processes such as turbulent entrainment and dynamic feedbacks can introduce a significant departure from the idealization we are considering. Full dynamical models account for dynamics feedbacks and several subgrid processes that could enhance or reduce the range of sensitivities that are demonstrated here. Nevertheless, the qualitative behavior of our main results, i.e., the dependency of the DSD sensitivity to the aerosol properties according to its position in the full parameter space, might not change. For example, Gettelman (2015) simulated several warm rain cases with the KiD model and climatological cases with a global model, using a double-moment microphysics scheme, in order to analyze the sensitivity of the ~~Amazon, due to biomass burning. These findings are also relevant given the current discussion about the importance of ultrafine aerosol particles in the development of deep convective clouds over the Amazon (Wang et al., 2016; Fan et al., 2018).~~ aerosol-cloud interaction to cloud microphysics. They found that the test in the KiD were consistent with the global sensitivity tests. This is an aspect we intend to study in a following work, to build on the present results.

6   Summary and conclusions

We illustrated the influence of the aerosol number concentration, the median radius and geometric standard deviation of the ~~aerosol size distribution~~PSD, and the hygroscopicity of the aerosols on the number concentration and effective diameter of droplets at the top of warm-phase clouds, for initial conditions typical of the Amazon. ~~Given the tested variations in the aerosol properties,~~ The sensitivities behaved accordingly with the relation between the supersaturaration and the aerosol availability, that determine the rate of aerosol activation, as described by Reutter et al. (2009). Nevertheless, in our analysis, the intensity of the droplet activation is mostly determined by the ~~cloud DSDs were found to behave as expected. Overall, when the nucleation is favored, an increase in the droplet number concentration is accompanied by a decrease in the droplet effective diameter. The effects of the investigated parameters were similar in all stages of the cloud-top evolution, except for the geometric standard deviation of the aerosol size distribution.Changes in the aerosol size distribution shape were more important in the earliest stages of the cloud –lower cloud-top heights– due to its dependence on the position of r_c with respect to the size distribution function~~amount of suitable-sized aerosols, i.e. the shape and median radius of the PSD, rather than on the total number concentration of aerosols.

We showed that the sensitivity to each aerosol characteristic varies as a function of the tested parameter and its value depends on the base value of the other parameters. The median radius of the aerosols is the most important parameter, from those analyzed, that influences the sensitivity to the others. ~~Based on its value, it is possible to define, inside Reutter et al. (2009) aerosol limited-regime, a concentration-limited regime, when other aerosol properties can be neglected, and a regime where all size distribution characteristics, total number concentration and hygroscopicity significantly influences the droplet number~~

~~concentration and effective diameter.~~ This expands the result of Ward et al. (2010) and states that w/N_a, or supersaturation-based regimes (Reutter et al., 2009), cannot fully predict the dependence of CCN activity, not only on the aerosol composition, but on all aerosol characteristics.

~~Despite using a simpler modeling approach, our results agree with previous studies, which assures the validity of our~~ ~~calculations . Thus,~~ Given the tested variations in the aerosol properties, the responses of the DSDs depend on the model assumptions regarding the entrainment and the treatment of the aerosol size distribution. This reinforces the importance of carefully considering the characteristics of the model when analyzing the responses to changes in aerosol loading in global or regional studies.

Overall, when the nucleation is favored, an increase in the droplet number concentration is accompanied by a decrease in the droplet effective diameter. However, since our sensitivity analysis involves the evolution of the cloud-top with time and height, the ~~application of these conclusions is not limited to models that use a similar representation of microphysics processes, but also to theoretical or experimental studies.~~ results are not directly comparable with previously reported sensitivity calculations at cloud-base. When a series of consecutive nucleation events is considered, such as those during the evolution of the cloud top, the intensity of the nucleation at certain time can modulate its intensity afterwards. The simulation with a bulk treatment of the aerosols constitutes an extreme case of slow aerosol depletion, where the responses of the nucleation to changes in the aerosol properties can impact the cloud-top in a more homogeneous way. That is the reason for the agreement in the sensitivity obtained from those simulations and previous cloud-base sensitivity calculations.

References

Albrecht, B. A.: Aerosols, Cloud Microphysics, and Fractional Cloudiness, Science, 245, 1227–1230, https://doi.org/10.1126/science.245.4923.1227, 1989.

Altaratz, O., Koren, I., Reisin, T., Kostinski, A., Feingold, G., Levin, Z., and Yin, Y.: Aerosols' influence on the interplay between condensation, evaporation and rain in warm cumulus cloud, Atmospheric Chemistry and Physics, 8, 15–24, https://doi.org/10.5194/acp-8-15-2008, 2008.

Andreae, M. O., Rosenfeld, D., Artaxo, P., Costa, A. A., Frank, G. P., Longo, K. M., and Silva-Dias, M. A. F.: Smoking Rain Clouds over the Amazon, Science, 303, 1337–1342, https://doi.org/10.1126/science.1092779, 2004.

Andreae, M. O., Afchine, A., Albrecht, R., Holanda, B. A., Artaxo, P., Barbosa, H. M. J., Borrmann, S., Cecchini, M. A., Costa, A., Dollner, M., Fütterer, D., Järvinen, E., Jurkat, T., Klimach, T., Konemann, T., Knote, C., Krämer, M., Krisna, T., Machado, L. A. T., Mertes, S., Minikin, A., Pöhlker, C., Pöhlker, M. L., Pöschl, U., Rosenfeld, D., Sauer, D., Schlager, H., Schnaiter, M., Schneider, J., Schulz, C., Spanu, A., Sperling, V. B., Voigt, C., Walser, A., Wang, J., Weinzierl, B., Wendisch, M., and Ziereis, H.: Aerosol characteristics and particle production in the upper troposphere over the Amazon Basin, Atmospheric Chemistry and Physics, 18, 921–961, https://doi.org/10.5194/acp-18-921-2018, 2018.

Anttila, T. and Kerminen, V.-M.: On the contribution of Aitken mode particles to cloud droplet populations at continental background areas – a parametric sensitivity study, Atmospheric Chemistry and Physics, 7, 4625–4637, https://doi.org/10.5194/acp-7-4625-2007, 2007.

Braga, R. C., Rosenfeld, D., Weigel, R., Jurkat, T., Andreae, M. O., Wendisch, M., Pöschl, U., Voigt, C., Mahnke, C., Borrmann, S., Albrecht, R. I., Molleker, S., Vila, D. A., Machado, L. A. T., and Grulich, L.: Further evidence for CCN aerosol concentrations determining the height of warm rain and ice initiation in convective clouds over the Amazon basin, Atmospheric Chemistry and Physics, 17, 14 433–14 456, https://doi.org/10.5194/acp-17-14433-2017, 2017.

Cecchini, M. A., Machado, L. A. T., Comstock, J. M., Mei, F., Wang, J., Fan, J., Tomlinson, J. M., Schmid, B., Albrecht, R., Martin, S. T., and Artaxo, P.: Impacts of the Manaus pollution plume on the microphysical properties of Amazonian warm-phase clouds in the wet season, Atmospheric Chemistry and Physics, 16, 7029–7041, https://doi.org/10.5194/acp-16-7029-2016, 2016.

Cecchini, M. A., Machado, L. A. T., Andreae, M. O., Martin, S. T., Albrecht, R. I., Artaxo, P., Barbosa, H. M. J., Borrmann, S., Fütterer, D., Jurkat, T., Mahnke, C., Minikin, A., Molleker, S., Pöhlker, M. L., Pöschl, U., Rosenfeld, D., Voigt, C., Weinzierl, B., and Wendisch, M.: Sensitivities of Amazonian clouds to aerosols and updraft speed, Atmospheric Chemistry and Physics, 17, 10 037–10 050, https://doi.org/10.5194/acp-17-10037-2017, 2017.

Charney, J. G. and Phillips, N. A.: Numerical integration of the quasi-geostrophic equations for barotropic and simple baroclinic flows, Journal of Meteorology, 10, 71–99, https://doi.org/10.1175/1520-0469(1953)010<0071:NIOTQG>2.0.CO;2, 1953.

Cubison, M. J., Ervens, B., Feingold, G., Docherty, K. S., Ulbrich, I. M., Shields, L., Prather, K., Hering, S., and Jimenez, J. L.: The influence of chemical composition and mixing state of Los Angeles urban aerosol on CCN number and cloud properties, Atmospheric Chemistry and Physics, 8, 5649–5667, https://doi.org/10.5194/acp-8-5649-2008, 2008.

Dusek, U., Frank, G. P., Hildebrandt, L., Curtius, J., Schneider, J., Walter, S., Chand, D., Drewnick, F., Hings, S., Jung, D., Borrmann, S., and Andreae, M. O.: Size Matters More Than Chemistry for Cloud-Nucleating Ability of Aerosol Particles, Science, 312, 1375–1378, https://doi.org/10.1126/science.1125261, 2006.

Ervens, B., Feingold, G., and Kreidenweis, S. M.: Influence of water-soluble organic carbon on cloud drop number concentration, Journal of Geophysical Research: Atmospheres, 110, https://doi.org/10.1029/2004JD005634, 2005.

Ervens, B., Cubison, M., Andrews, E., Feingold, G., Ogren, J. A., Jimenez, J. L., DeCarlo, P., and Nenes, A.: Prediction of cloud condensation nucleus number concentration using measurements of aerosol size distributions and composition and light scattering enhancement due to humidity, Journal of Geophysical Research: Atmospheres, 112, https://doi.org/10.1029/2006JD007426, 2007.

Fan, J., Zhang, R., Li, G., Tao, W.-K., and Li, X.: Simulations of cumulus clouds using a spectral microphysics cloud-resolving model, Journal of Geophysical Research: Atmospheres, 112, https://doi.org/10.1029/2006JD007688, 2007.

Fan, J., Rosenfeld, D., Zhang, Y., Giangrande, S. E., Li, Z., Machado, L. A. T., Martin, S. T., Yang, Y., Wang, J., Artaxo, P., Barbosa, H. M. J., Braga, R. C., Comstock, J. M., Feng, Z., Gao, W., Gomes, H. B., Mei, F., Pöhlker, C., Pöhlker, M. L., Pöschl, U., and de Souza, R. A. F.: Substantial convection and precipitation enhancements by ultrafine aerosol particles, Science, 359, 411–418, https://doi.org/10.1126/science.aan8461, 2018.

Feingold, G.: Modeling of the first indirect effect: Analysis of measurement requirements, Geophysical Research Letters, 30, https://doi.org/10.1029/2003GL017967, 2003.

Feingold, G., Tzivion, S., and Leviv, Z.: Evolution of Raindrop Spectra. Part I: Solution to the Stochastic Collection/Breakup Equation Using the Method of Moments, Journal of the Atmospheric Sciences, 45, 3387–3399, https://doi.org/10.1175/1520-0469(1988)045<3387:EORSPI>2.0.CO;2, 1988.

Freud, E., Rosenfeld, D., and Kulkarni, J. R.: Resolving both entrainment-mixing and number of activated CCN in deep convective clouds, Atmospheric Chemistry and Physics, 11, 12 887–12 900, https://doi.org/10.5194/acp-11-12887-2011, 2011.

Gettelman, A.: Putting the clouds back in aerosol–cloud interactions, Atmospheric Chemistry and Physics, 15, 12 397–12 411, https://doi.org/10.5194/acp-15-12397-2015, https://www.atmos-chem-phys.net/15/12397/2015/, 2015.

Gonçalves, W. A., Machado, L. A. T., and Kirstetter, P.-E.: Influence of biomass aerosol on precipitation over the Central Amazon: an observational study, Atmospheric Chemistry and Physics, 15, 6789–6800, https://doi.org/10.5194/acp-15-6789-2015, 2015.

Gunthe, S. S., King, S. M., Rose, D., Chen, Q., Roldin, P., Farmer, D. K., Jimenez, J. L., Artaxo, P., Andreae, M. O., Martin, S. T., and Pöschl, U.: Cloud condensation nuclei in pristine tropical rainforest air of Amazonia: size-resolved measurements and modeling of atmospheric aerosol composition and CCN activity, Atmospheric Chemistry and Physics, 9, 7551–7575, https://doi.org/10.5194/acp-9-7551-2009, 2009.

Heiblum, R. H., Altaratz, O., Koren, I., Feingold, G., Kostinski, A. B., Khain, A. P., Ovchinnikov, M., Fredj, E., Dagan, G., Pinto, L., Yaish, R., and Chen, Q.: Characterization of cumulus cloud fields using trajectories in the center of gravity versus water mass phase space: 2. Aerosol effects on warm convective clouds, Journal of Geophysical Research: Atmospheres, 121, 6356–6373, https://doi.org/10.1002/2015JD024193, 2016.

Hill, A., Dobbie, S., and Yin, Y.: The impact of aerosols on non-precipitating marine stratocumulus. I: Model description and prediction of the indirect effect, Quarterly Journal of the Royal Meteorological Society: A journal of the atmospheric sciences, applied meteorology and physical oceanography, 134, 1143–1154, 2008.

Hudson, J. G.: Variability of the relationship between particle size and cloud-nucleating ability, Geophysical Research Letters, 34, https://doi.org/10.1029/2006GL028850, 2007.

Ivanova, E. T.: Method of parameterizing the condensation process of droplet growth in numerical models, Izv. Akad. Sci. USSR Atmos. Ocean Phys., 13, 821–826, 1977.

Karydis, V. A., Capps, S. L., Russell, A. G., and Nenes, A.: Adjoint sensitivity of global cloud droplet number to aerosol and dynamical parameters, Atmospheric Chemistry and Physics, 12, 9041–9055, https://doi.org/10.5194/acp-12-9041-2012, 2012.

Khain, A., Rosenfeld, D., and Pokrovsky, A.: Aerosol impact on the dynamics and microphysics of deep convective clouds, Quarterly Journal of the Royal Meteorological Society, 131, 2639–2663, https://doi.org/10.1256/qj.04.62, 2005.

Kogan, Y., Khairoutdinov, M., Lilly, D., Kogan, Z., and Liu, Q.: Modeling of stratocumulus cloud layers in a large eddy simulation model with explicit microphysics, Journal of the atmospheric sciences, 52, 2923–2940, 1995.

5   Kogan, Y. L.: The simulation of a convective cloud in a 3-D model with explicit microphysics. Part I: Model description and sensitivity experiments, Journal of the atmospheric sciences, 48, 1160–1189, 1991.

Koren, I., Feingold, G., and Remer, L. A.: The invigoration of deep convective clouds over the Atlantic: aerosol effect, meteorology or retrieval artifact?, Atmospheric Chemistry and Physics, 10, 8855–8872, https://doi.org/10.5194/acp-10-8855-2010, 2010.

Lebo, Z. J. and Seinfeld, J. H.: A continuous spectral aerosol-droplet microphysics model, Atmospheric Chemistry and Physics, 11, 12 297–

10   12 316, https://doi.org/10.5194/acp-11-12297-2011, https://www.atmos-chem-phys.net/11/12297/2011/, 2011.

Lee, S. S., Donner, L. J., Phillips, V. T. J., and Ming, Y.: Examination of aerosol effects on precipitation in deep convective clouds during the 1997 ARM summer experiment, Quarterly Journal of the Royal Meteorological Society, 134, 1201–1220, https://doi.org/10.1002/qj.287, 2008.

Leonard, B., MacVean, M., and Lock, A.: Positivity-preserving numerical schemes for multidimensional advection, Technical Report, NASA,

15   United States, 64 pp., 1993.

Leroy, D., Wobrock, W., and Flossmann, A. I.: On the influence of the treatment of aerosol particles in different bin microphysical models: A comparison between two different schemes, Atmospheric Research, 85, 269 – 287, https://doi.org/https://doi.org/10.1016/j.atmosres.2007.01.003, 2007.

Li, Z., Niu, F., Fan, J., Liu, Y., Rosenfeld, D., and Ding, Y.: Long-term impacts of aerosols on the vertical development of clouds and

20   precipitation, Nature Geoscience, 4, 888–894, https://doi.org/10.1038/NGEO1313, 2011.

Lorenz, E. N.: Energy and Numerical Weather Prediction, Tellus, 12, 364–373, https://doi.org/10.3402/tellusa.v12i4.9420, 1960.

Machado, L. A. T., Silva Dias, M. A. F., Morales, C., Fisch, G., Vila, D., Albrecht, R., Goodman, S. J., Calheiros, A. J. P., Biscaro, T., Kummerow, C., Cohen, J., Fitzjarrald, D., Nascimento, E. L., Sakamoto, M. S., Cunningham, C., Chaboureau, J.-P., Petersen, W. A., Adams, D. K., Baldini, L., Angelis, C. F., Sapucci, L. F., Salio, P., Barbosa, H. M. J., Landulfo, E., Souza, R. A. F., Blakeslee, R. J.,

25   Bailey, J., Freitas, S., Lima, W. F. A., and Tokay, A.: The Chuva Project: How Does Convection Vary across Brazil?, Bulletin of the American Meteorological Society, 95, 1365–1380, https://doi.org/10.1175/BAMS-D-13-00084.1, 2014.

Martin, S. T., Andreae, M. O., Artaxo, P., Baumgardner, D., Chen, Q., Goldstein, A. H., Guenther, A., Heald, C. L., Mayol-Bracero, O. L., Mc-Murry, P. H., Pauliquevis, T., Pöschl, U., Prather, K. A., Roberts, G. C., Saleska, S. R., Silva Dias, M. A., Spracklen, D. V., Swietlicki, E., and Trebs, I.: Sources and properties of Amazonian aerosol particles, Reviews of Geophysics, 48, https://doi.org/10.1029/2008RG000280,

30   2010.

McFiggans, G., Artaxo, P., Baltensperger, U., Coe, H., Facchini, M. C., Feingold, G., Fuzzi, S., Gysel, M., Laaksonen, A., Lohmann, U., Mentel, T. F., Murphy, D. M., O'Dowd, C. D., Snider, J. R., and Weingartner, E.: The effect of physical and chemical aerosol properties on warm cloud droplet activation, Atmospheric Chemistry and Physics, 6, 2593–2649, https://doi.org/10.5194/acp-6-2593-2006, 2006.

Mechem, D. B. and Kogan, Y. L.: A Bulk Parameterization of Giant CCN, Journal of the Atmospheric Sciences, 65, 2458–2466,

35   https://doi.org/10.1175/2007JAS2502.1, 2008.

Petters, M. D. and Kreidenweis, S. M.: A single parameter representation of hygroscopic growth and cloud condensation nucleus activity, Atmospheric Chemistry and Physics, 7, 1961–1971, https://doi.org/10.5194/acp-7-1961-2007, 2007.

Pinsky, M. and Khain, A.: Theoretical analysis of mixing in liquid clouds – Part IV: DSD evolution and mixing diagrams, Atmospheric Chemistry and Physics, 18, 3659–3676, https://doi.org/10.5194/acp-18-3659-2018, 2018.

Pinsky, M., Khain, A., Korolev, A., and Magaritz-Ronen, L.: Theoretical investigation of mixing in warm clouds – Part 2: Homogeneous mixing, Atmospheric Chemistry and Physics, 16, 9255–9272, https://doi.org/10.5194/acp-16-9255-2016, 2016.

5 Pöhlker, M. L., Pöhlker, C., Ditas, F., Klimach, T., Hrabe de Angelis, I., Araújo, A., Brito, J., Carbone, S., Cheng, Y., Chi, X., Ditz, R., Gunthe, S. S., Kesselmeier, J., Könemann, T., Lavrič, J. V., Martin, S. T., Mikhailov, E., Moran-Zuloaga, D., Rose, D., Saturno, J., Su, H., Thalman, R., Walter, D., Wang, J., Wolff, S., Barbosa, H. M. J., Artaxo, P., Andreae, M. O., and Pöschl, U.: Long-term observations of cloud condensation nuclei in the Amazon rain forest – Part 1: Aerosol size distribution, hygroscopicity, and new model parametrizations for CCN prediction, Atmospheric Chemistry and Physics, 16, 15 709–15 740, https://doi.org/10.5194/acp-16-15709-2016, 2016.

10 Pruppacher, H. R. and Klett, J. D.: Microphysics of Clouds and Precipitation: Reprinted 1980, Springer Science & Business Media, 2012.

Quinn, P. K., Bates, T. S., Coffman, D. J., and Covert, D. S.: Influence of particle size and chemistry on the cloud nucleating properties of aerosols, Atmospheric Chemistry and Physics, 8, 1029–1042, https://doi.org/10.5194/acp-8-1029-2008, 2008.

Reid, J. S., Hobbs, P. V., Rangno, A. L., and Hegg, D. A.: Relationships between cloud droplet effective radius, liquid water content, and droplet concentration for warm clouds in Brazil embedded in biomass smoke, Journal of Geophysical Research: Atmospheres, 104, 6145–6153, https://doi.org/10.1029/1998JD200119, 1999.

15

Reisin, T. G., Yin, Y., Levin, Z., and Tzivion, S.: Development of giant drops and high-reflectivity cores in Hawaiian clouds: numerical simulations using a kinematic model with detailed microphysics, Atmospheric Research, 45, 275 – 297, https://doi.org/10.1016/S0169-8095(97)00081-1, 1998.

Reutter, P., Su, H., Trentmann, J., Simmel, M., Rose, D., Gunthe, S. S., Wernli, H., Andreae, M. O., and Pöschl, U.: Aerosol- and updraft-limited regimes of cloud droplet formation: influence of particle number, size and hygroscopicity on the activation of cloud condensation nuclei (CCN), Atmospheric Chemistry and Physics, 9, 7067–7080, https://doi.org/10.5194/acp-9-7067-2009, 2009.

20

Rissman, T. A., Nenes, A., and Seinfeld, J. H.: Chemical Amplification (or Dampening) of the Twomey Effect: Conditions Derived from Droplet Activation Theory, Journal of the Atmospheric Sciences, 61, 919–930, https://doi.org/10.1175/1520-0469(2004)061<0919:CAODOT>2.0.CO;2, 2004.

25 Roesler, E. L. and Penner, J. E.: Can global models ignore the chemical composition of aerosols?, Geophysical Research Letters, 37, https://doi.org/10.1029/2010GL044282, 2010.

Rose, D., Nowak, A., Achtert, P., Wiedensohler, A., Hu, M., Shao, M., Zhang, Y., Andreae, M. O., and Pöschl, U.: Cloud condensation nuclei in polluted air and biomass burning smoke near the mega-city Guangzhou, China – Part 1: Size-resolved measurements and implications for the modeling of aerosol particle hygroscopicity and CCN activity, Atmospheric Chemistry and Physics, 10, 3365–3383,

30 https://doi.org/10.5194/acp-10-3365-2010, 2010.

Rosenfeld, D., Lohmann, U., Raga, G. B., O'Dowd, C. D., Kulmala, M., Fuzzi, S., Reissell, A., and Andreae, M. O.: Flood or Drought: How Do Aerosols Affect Precipitation?, Science, 321, 1309–1313, https://doi.org/10.1126/science.1160606, 2008.

Rotach, M. W. and Zardi, D.: On the boundary-layer structure over highly complex terrain: Key findings from MAP, Quarterly Journal of the Royal Meteorological Society, 133, 937–948, https://doi.org/10.1002/qj.71, 2007.

35 Sánchez Gácita, M., Longo, K. M., Freire, J. L. M., Freitas, S. R., and Martin, S. T.: Impact of mixing state and hygroscopicity on CCN activity of biomass burning aerosol in Amazonia, Atmospheric Chemistry and Physics, 17, 2373–2392, https://doi.org/10.5194/acp-17-2373-2017, 2017.

Seifert, A. and Beheng, K. D.: A two-moment cloud microphysics parameterization for mixed-phase clouds. Part 2: Maritime vs. continental deep convective storms, Meteorology and Atmospheric Physics, 92, 67–82, https://doi.org/10.1007/s00703-005-0113-3, 2006.

Shipway, B. J. and Hill, A. A.: Diagnosis of systematic differences between multiple parametrizations of warm rain microphysics using a kinematic framework, Quarterly Journal of the Royal Meteorological Society, 138, 2196–2211, https://doi.org/10.1002/qj.1913, 2012.

5   Stevens, B., Feingold, G., Cotton, W. R., and Walko, R. L.: Elements of the Microphysical Structure of Numerically Simulated Nonprecipitating Stratocumulus, Journal of the Atmospheric Sciences, 53, 980–1006, https://doi.org/10.1175/1520-0469(1996)053<0980:EOTMSO>2.0.CO;2, 1996.

Sun, J., Leighton, H., Yau, M. K., and Ariya, P.: Numerical evidence for cloud droplet nucleation at the cloud-environment interface, Atmospheric Chemistry and Physics, 12, 12 155–12 164, https://doi.org/10.5194/acp-12-12155-2012, 2012.

10   Twomey, S.: Pollution and the planetary albedo, Atmospheric Environment (1967), 8, 1251 – 1256, https://doi.org/10.1016/0004-6981(74)90004-3, 1974.

Tzivion, S., Feingold, G., and Levin, Z.: An Efficient Numerical Solution to the Stochastic Collection Equation, Journal of the Atmospheric Sciences, 44, 3139–3149, https://doi.org/10.1175/1520-0469(1987)044<3139:AENSTT>2.0.CO;2, 1987.

Tzivion, S., Feingold, G., and Levin, Z.: The Evolution of Raindrop Spectra. Part II: Collisional Collection/Breakup and Evaporation in a
15   Rainshaft, Journal of the Atmospheric Sciences, 46, 3312–3328, https://doi.org/10.1175/1520-0469(1989)046<3312:TEORSP>2.0.CO;2, 1989.

Wang, J., Krejci, R., Giangrande, S., Kuang, C., Barbosa, H. M. J., Brito, J., Carbone, S., Chi, X., Comstock, J., Ditas, F., Lavric, J., Manninen, H. E., Mei, F., Moran-Zuloaga, D., Pöhlker, C., Pöhlker, M. L., Saturno, J., Schmid, B., Souza, R. A. F., Springston, S. R., Tomlinson, J. M., Toto, T., Walter, D., Wimmer, D., Smith, J. N., Kulmala, M., Machado, L. A. T., Artaxo, P., Andreae, M. O., Petäjä,
20   T., and Martin, S. T.: Amazon boundary layer aerosol concentration sustained by vertical transport during rainfall, Nature, 539, 416–419, https://doi.org/10.1038/nature19819, 2016.

Ward, D. S., Eidhammer, T., Cotton, W. R., and Kreidenweis, S. M.: The role of the particle size distribution in assessing aerosol composition effects on simulated droplet activation, Atmospheric Chemistry and Physics, 10, 5435–5447, https://doi.org/10.5194/acp-10-5435-2010, 2010.

25   Wendisch, M., Pöschl, U., Andreae, M. O., Machado, L. A. T., Albrecht, R., Schlager, H., Rosenfeld, D., Martin, S. T., Abdelmonem, A., Afchine, A., Araùjo, A. C., Artaxo, P., Aufmhoff, H., Barbosa, H. M. J., Borrmann, S., Braga, R., Buchholz, B., Cecchini, M. A., Costa, A., Curtius, J., Dollner, M., Dorf, M., Dreiling, V., Ebert, V., Ehrlich, A., Ewald, F., Fisch, G., Fix, A., Frank, F., Fütterer, D., Heckl, C., Heidelberg, F., Hüneke, T., Jäkel, E., Järvinen, E., Jurkat, T., Kanter, S., Kästner, U., Kenntner, M., Kesselmeier, J., Klimach, T., Knecht, M., Kohl, R., Kölling, T., Krämer, M., Krüger, M., Krisna, T. C., Lavric, J. V., Longo, K., Mahnke, C., Manzi, A. O., Mayer, B.,
30   Mertes, S., Minikin, A., Molleker, S., Münch, S., Nillius, B., Pfeilsticker, K., Pöhlker, C., Roiger, A., Rose, D., Rosenow, D., Sauer, D., Schnaiter, M., Schneider, J., Schulz, C., de Souza, R. A. F., Spanu, A., Stock, P., Vila, D., Voigt, C., Walser, A., Walter, D., Weigel, R., Weinzierl, B., Werner, F., Yamasoe, M. A., Ziereis, H., Zinner, T., and Zöger, M.: ACRIDICON–CHUVA Campaign: Studying Tropical Deep Convective Clouds and Precipitation over Amazonia Using the New German Research Aircraft HALO, Bulletin of the American Meteorological Society, 97, 1885–1908, https://doi.org/10.1175/BAMS-D-14-00255.1, 2016.

35   Yin, Y., Levin, Z., Reisin, T., and Tzivion, S.: Seeding Convective Clouds with Hygroscopic Flares: Numerical Simulations Using a Cloud Model with Detailed Microphysics, Journal of Applied Meteorology, 39, 1460–1472, https://doi.org/10.1175/1520-0450(2000)039<1460:SCCWHF>2.0.CO;2, 2000a.

Yin, Y., Levin, Z., Reisin, T. G., and Tzivion, S.: The effects of giant cloud condensation nuclei on the development of precipitation in convective clouds — a numerical study, Atmospheric Research, 53, 91 – 116, https://doi.org/https://doi.org/10.1016/S0169-8095(99)00046-0, 2000b.

YIN, Y., CARSLAW, K. S., and FEINGOLD, G.: Vertical transport and processing of aerosols in a mixed-phase convective cloud and the feedback on cloud development, Quarterly Journal of the Royal Meteorological Society, 131, 221–245, https://doi.org/10.1256/qj.03.186, 2005.

5
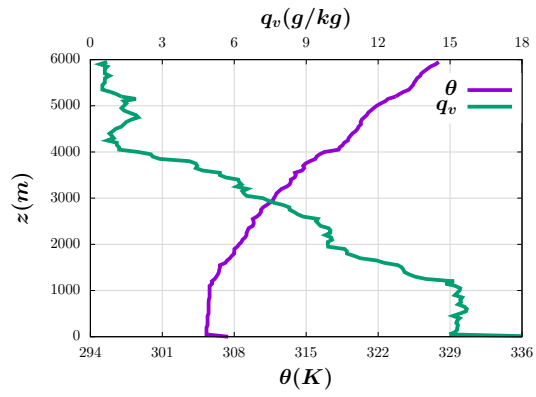
Figure 1. ~~Model configuration: (a)~~ Vertical profiles employed as initial conditions ~~and (b) prescribed field of vertical velocity~~ in the simulations
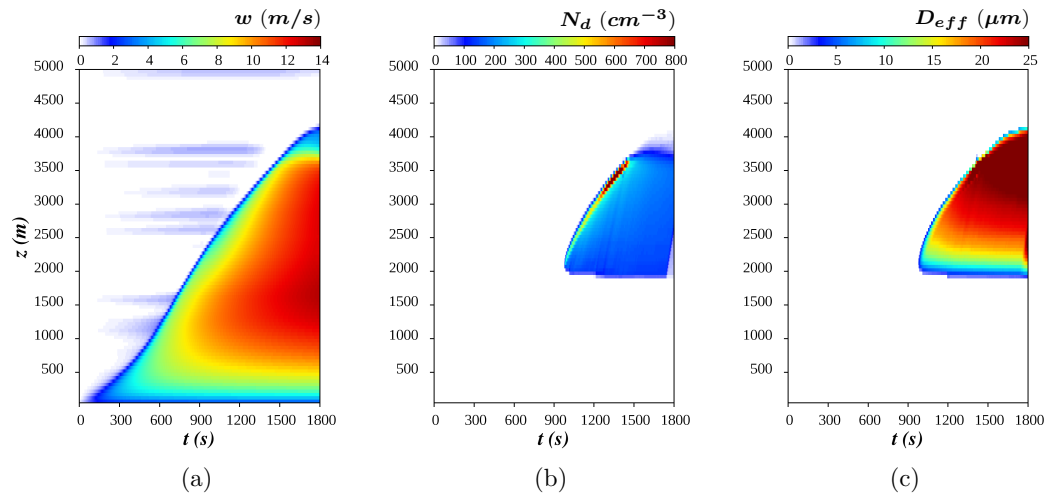
Figure 2. Evolution of ~~N_d~~ w (~~cm^{-3}~~ m/s), ~~D_{eff}~~ N_d (~~μ m~~ cm^{-3}) and ~~q_c~~ D_{eff} (~~g/kg~~ μ m) in the simulation. ~~The black lines represent cloud-top.~~
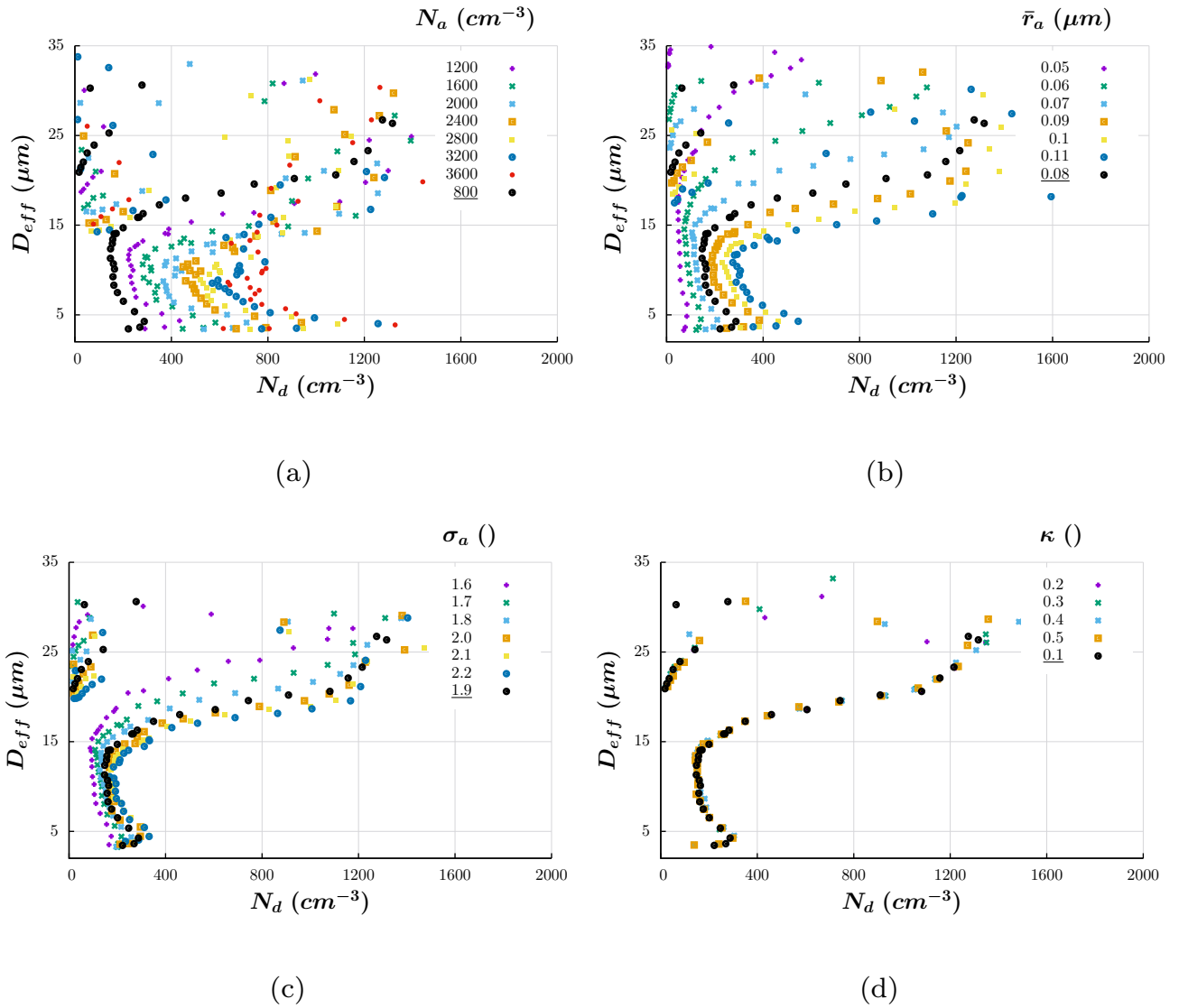
Figure 3. Illustration of the sensitivity of cloud-top bulk properties to (a) the aerosol number concentration (cm^{-3}), (b) the median radius of the ~~aerosol size distribution~~ PSD (~~μm~~ μ m), (c) the geometric standard deviation of the ~~aerosol size distribution~~ PSD (~~dimensionless~~), and (d) the aerosol hygroscopicity (~~dimensionless~~). The markers represent the averaged DSDs for the time steps when the cloud top remains at the same model level during its growth. The colors distinguish between simulations using different values of the parameter specified at the top of the graphs. The control simulation is represented by black markers in the figures.
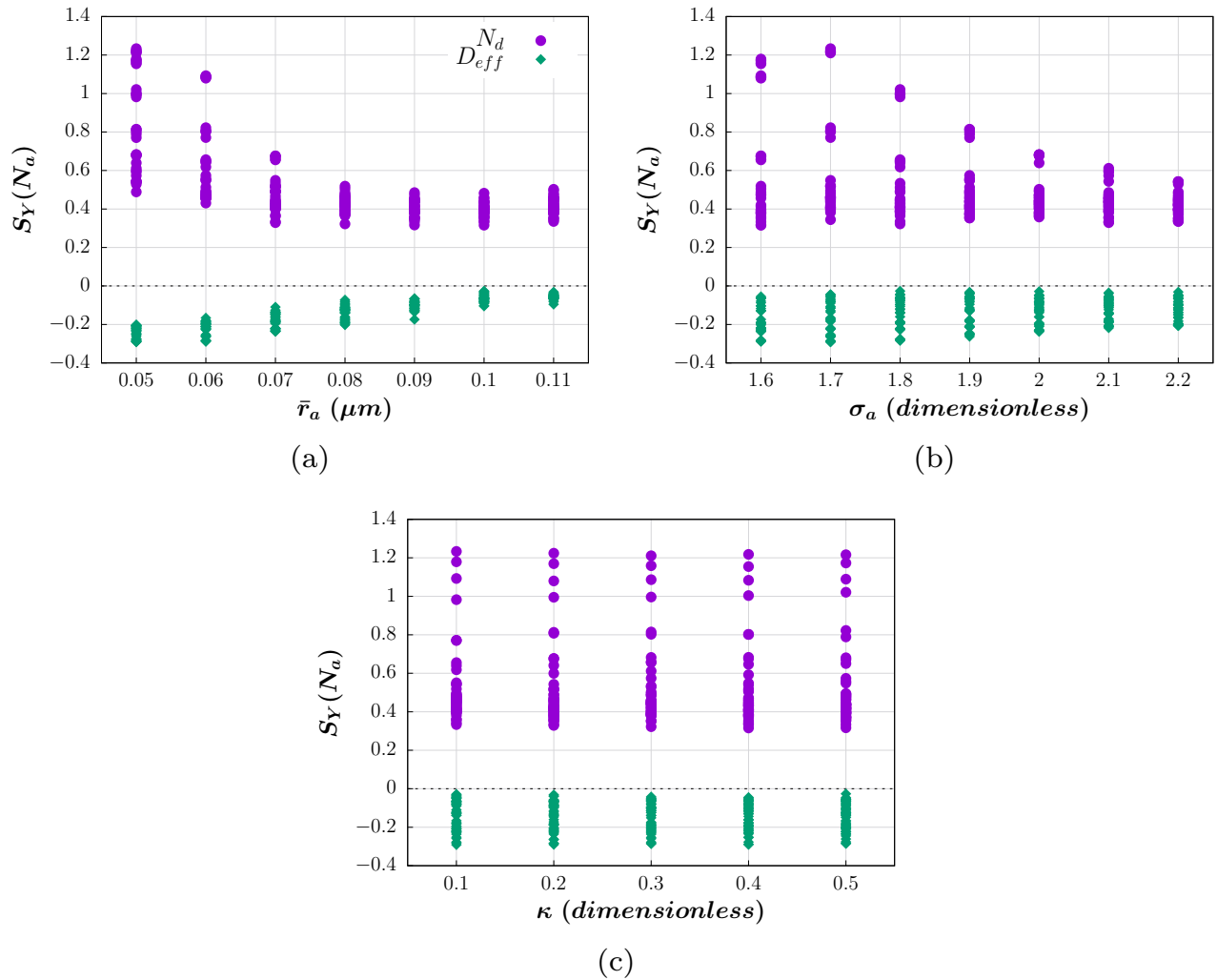
Figure 4. Sensitivities of the droplet number concentration and effective diameter to the aerosol number concentration ($S_Y(N_a)$) as a function of (a) the median radius of the ~~aerosol size distribution~~ PSD (μm ~~μ m~~), (b) the geometric standard deviation of the ~~aerosol size distribution~~ PSD (~~dimensionless~~) and (c) the aerosol hygroscopicity (~~dimensionless~~).
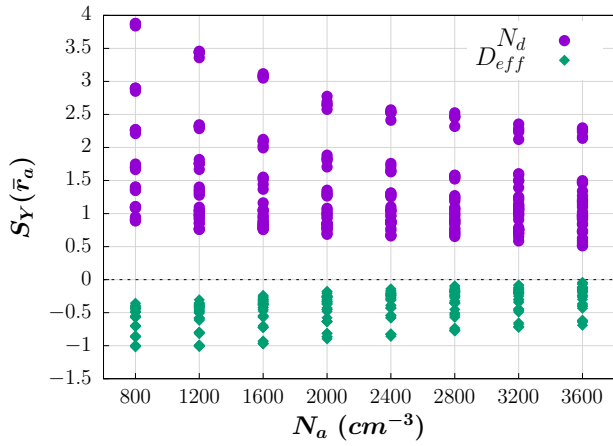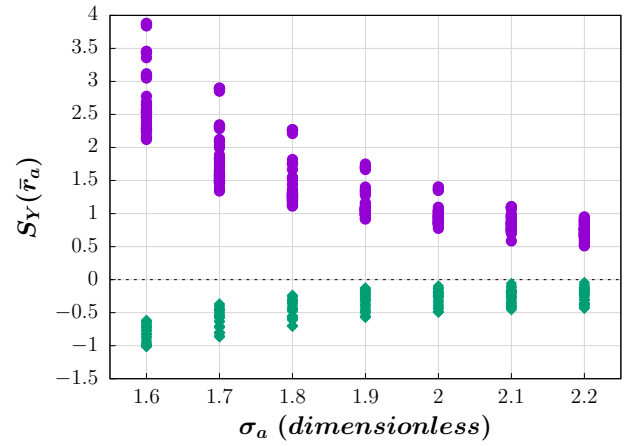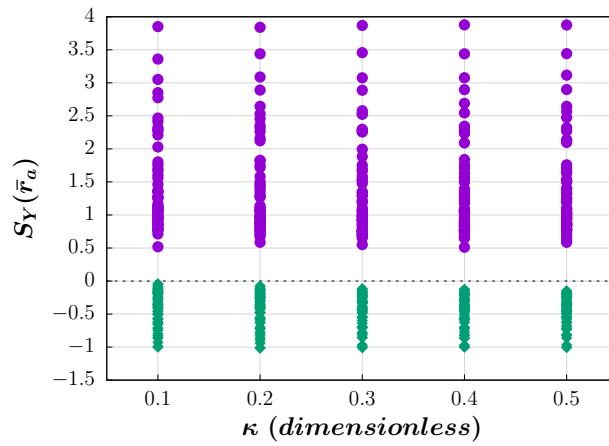
Figure 5. Sensitivities of the droplet number concentration and effective diameter to the median radius of the ~~aerosol size distribution~~ PSD ($S_Y(\bar{r}_a)$) as a function of (a) the aerosol number concentration (cm^{-3}), (b) the geometric standard deviation of the ~~aerosol size distribution~~ PSD (~~dimensionless~~) and (c) the aerosol hygroscopicity (~~dimensionless~~).
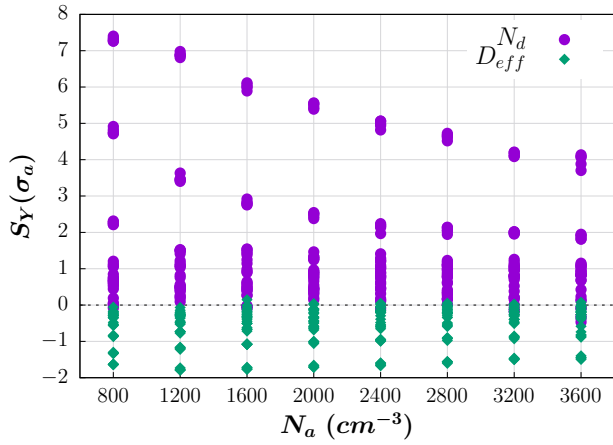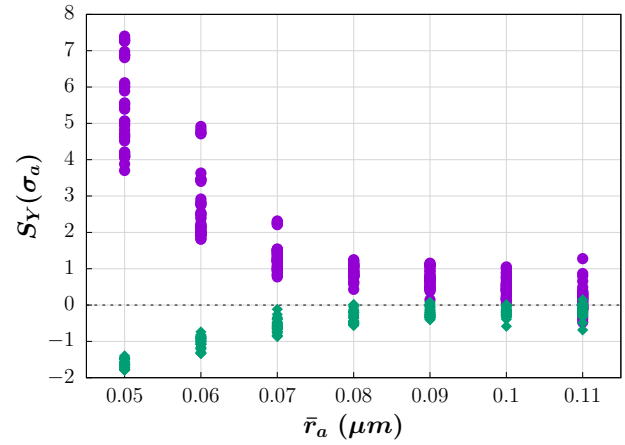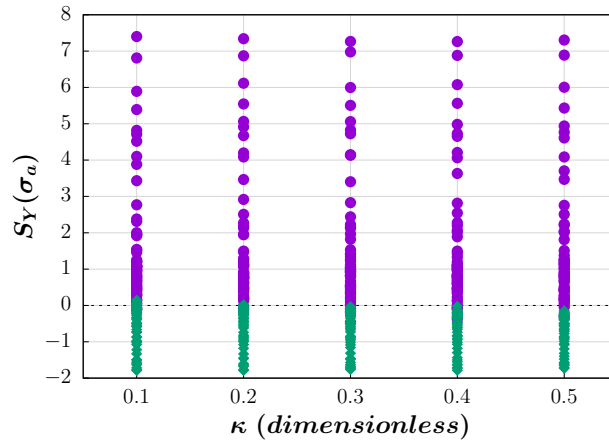
Figure 6. Sensitivities of the droplet number concentration and effective diameter to the geometric standard deviation of the ~~aerosol size distribution~~ PSD ($S_Y(\sigma_a)$) as a function of (a) the aerosol number concentration (cm^{-3}), (b) the median radius of the ~~aerosol size distribution~~ PSD (~~μm~~ μ m) and (c) the aerosol hygroscopicity (~~dimensionless~~).
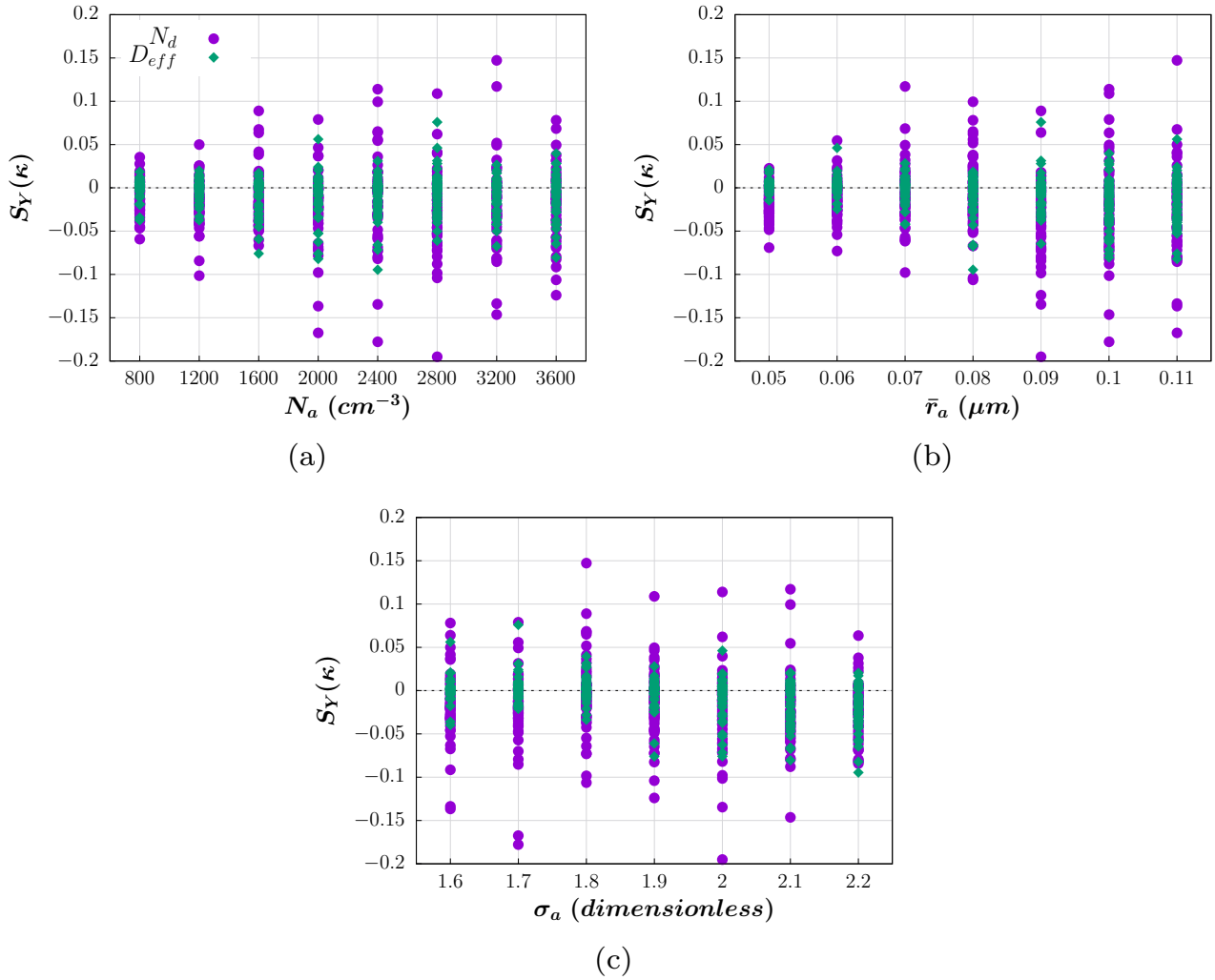
Figure 7. Sensitivities of the droplet number concentration and effective diameter to the aerosol hygroscopicity ($S_Y(\kappa)$) as a function of (a) the aerosol number concentration (cm^{-3}), (b) the median radius of the ~~aerosol size distribution~~ PSD (μm μ m) and (c) the geometric standard deviation of the ~~aerosol size distribution~~ PSD (dimensionless).
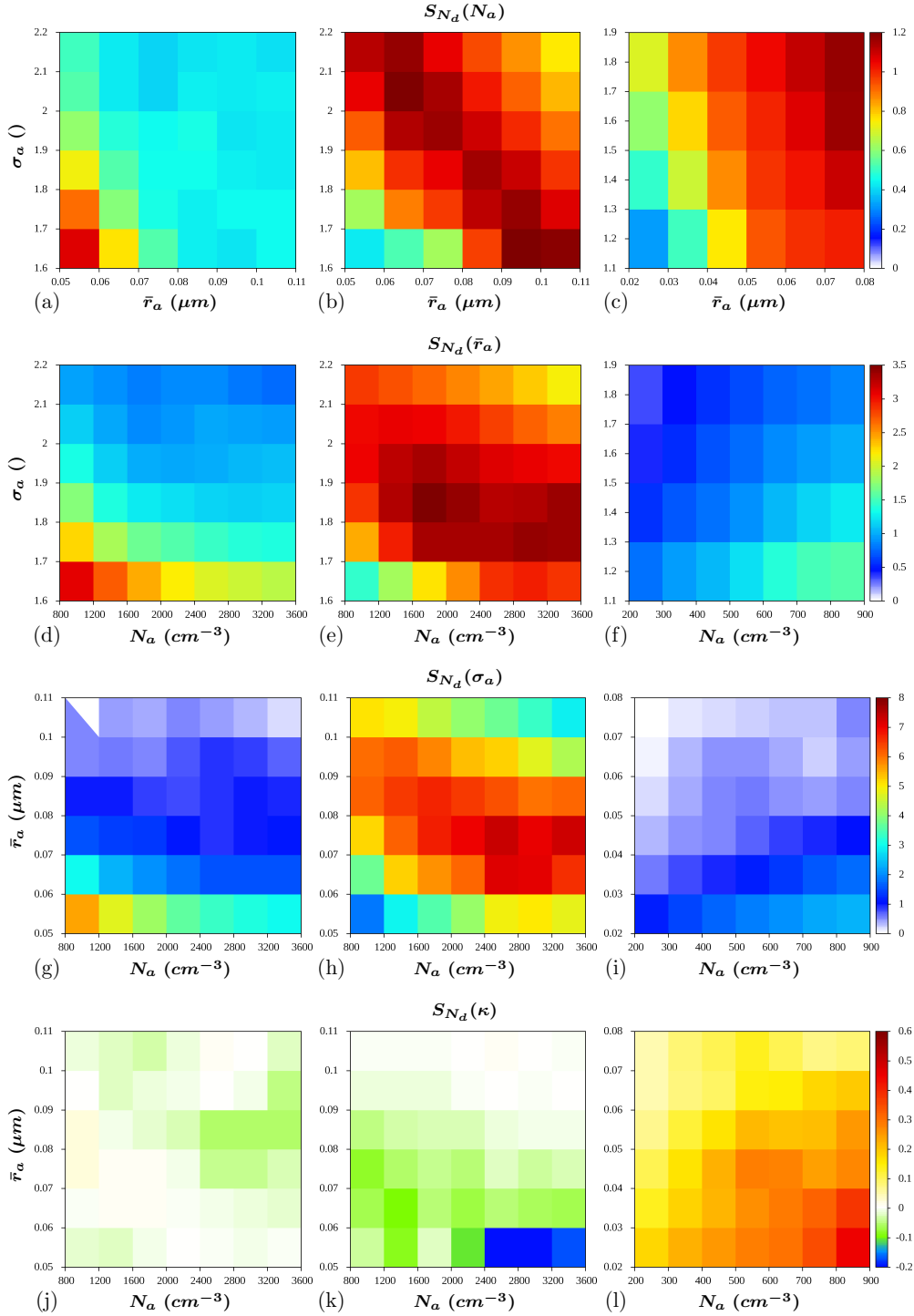
Figure 8. ~~Mean and standard deviation~~ <u>Sensitivity</u> of $\bar{N}_d$ <u>to</u> the ~~time-averaged values~~ <u>aerosol properties in three different configurations</u> of ~~N_d~~ <u>the model: with entrainment</u> and ~~D_{eff}~~ <u>at</u> <u>bins for</u> the ~~cloud top~~ <u>aerosols (a,d,g,j), without entrainment (b,e,h,k) and without bins for</u> ~~each simulation.~~<u>the aerosol (c,f,i,l)</u>

31
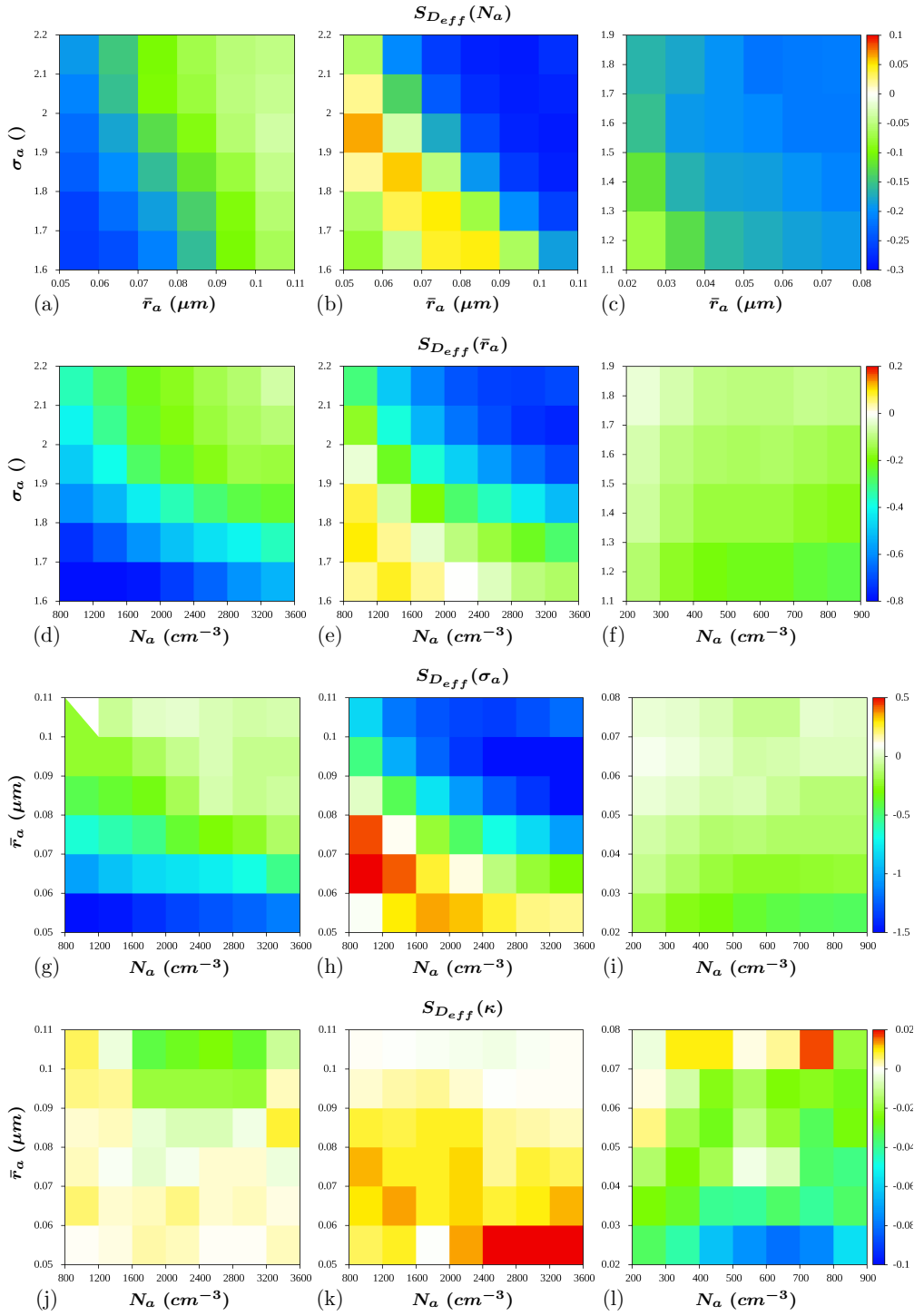
Figure 9. Sensitivity of $\bar{D}_{eff}$ to the aerosol properties in three different configurations of the model: with entrainment and bins for the aerosols (a,d,g,j), without entrainment (b,e,h,k) and without bins for the aerosol (c,f,i,l)
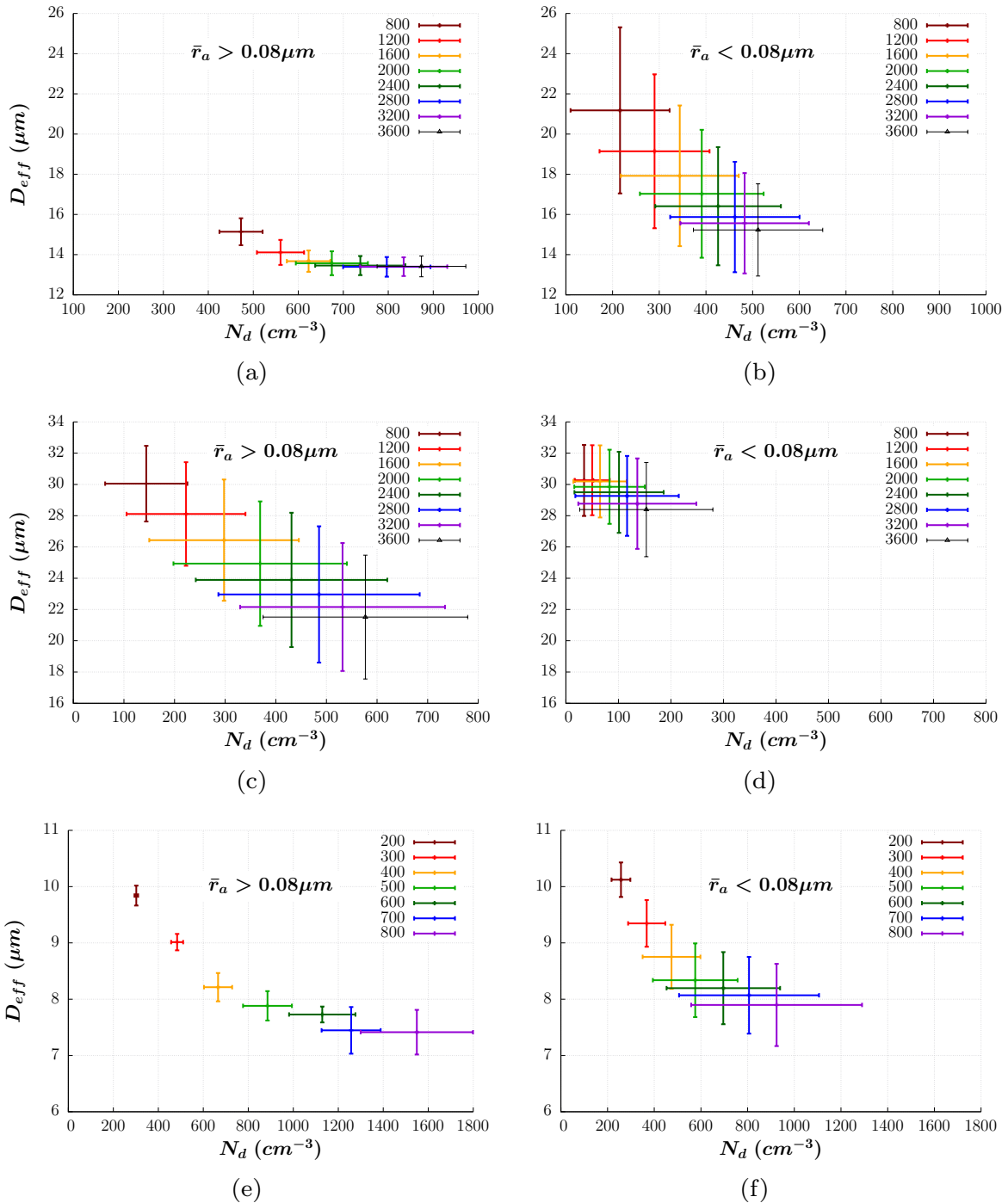
Figure 10. Mean and standard deviation of $\bar{N}_d$ and $\bar{D}_{eff}$ at cloud top from the simulations with entrainment and bins for the aerosols (a,b), without entrainment (c,d) and without bins for the aerosol (e,f).